Regulation of target proteins by small ubiquitin-like modifiers

Xiao, Z.

Chapter 3
Proteomics reveals global regulation of protein SUMOylation by ATM and ATR kinases in replication stress

Stephanie Munk[1,2,4], Jón Otti Sigurðsson[1,4], Zhenyu Xiao[3,4], Tanveer Singh Batth[1], Giulia Franciosa[1], Louise von Stechow[1], Andres Joaquin Lopez-Contreras[2], Alfred Cornelis Otto Vertegaal[3*], Jesper Velgaard Olsen[1,5*]

[1]Proteomics program, Novo Nordisk Foundation Center for Protein Research, Faculty of Health and Medical Sciences, University of Copenhagen, 2200 Copenhagen, Denmark.
[2]Center for Chromosome Stability and Center for Healthy Aging, Institute for Cellular and Molecular Medicine, Faculty of Health and Medical Sciences, University of Copenhagen, 2200 Copenhagen, Denmark.
[3]Department of Molecular Cell Biology, Leiden University Medical Center, 2300 RC Leiden, The Netherlands.
[4]These authors contributed equally
[5]Lead Contact

*Correspondence should be directed to J.V.O (jesper.olsen@cpr.ku.dk) and A.C.O.V (A.C.O.Vertegaal@lumc.nl)

Chapter 3 has been published in **Cell reports**
Cell Rep. 2017 Oct 10;21(2):546-558. doi: 10.1016/j.celrep.2017.09.059.
Supplementary Tables are available online

Summary

The mechanisms that protect eukaryotic DNA during the cumbersome task of replication depend on the precise coordination of several post-translational modifications (PTMs)-based signaling networks. Phosphorylation is a well-known regulator of the replication stress response and recently an essential role for SUMO (small ubiquitin-like modifiers) has also been established. Here we investigate the global interplay between phosphorylation and SUMOylation in response to replication stress. Using the latest SUMO- and phospho-proteomics technologies, we identified thousands of regulated modification sites. We found co-regulation of central DNA damage and replication stress responders of which the ATR activating factor, TOPBP1 was the most highly regulated. Using pharmacological inhibition of the apical DNA damage response kinases, ATR and ATM, we found these to regulate global protein SUMOylation in the protein networks that protect DNA upon replication stress and fork breakage. Combined, we uncovered integration between phosphorylation and SUMOylation in the cellular systems that protect DNA integrity.

1 Introduction

DNA replication is a tremendously challenging, time consuming and vital task for eukaryotic organisms. The maintenance of genomic integrity during this process is challenged by endogenous and exogenous factors that cause replication forks to slow, stall and in extreme cases this leads to DNA breakage (Halazonetis et al., 2008). Cells are equipped with a complex DNA damage response (DDR), consisting of protein networks that enable them to cope with replication stress (RS), and a malfunction in these systems can result in genomic instability and oncogenesis (Jackson and Bartek, 2009). These protective signaling pathways require the precise spatial and temporal coordination of DDR components, which is achieved by dynamic and specific post-translational modifications (PTMs) (Polo and Jackson, 2011). In particular, protein phosphorylation is the well-established driver of the RS response, with the ATR (Ataxia telangiectasia and Rad3-related protein) kinase functioning as the key initiator and orchestrator (López-Contreras and Fernandez-Capetillo, 2010; Shiloh, 2001). Depletion of this central kinase leads to replication fork breakage and genomic instability, thereby instigating a phosphorylation response mounted by the ATM (Ataxia telangiectasia mutated) kinase, which mediates repair and checkpoint activation upon double strand DNA breaks (DSBs) (Murga et al., 2009; Smith et al., 2010). ATM and ATR belong to the same atypical serine/threonine kinase family (the PIKK-related kinases) with similar substrate sequence specificity (Kim et al., 2009), yet they have unique triggers. While ATR responds to the accumulation of single stranded DNA (ssDNA) and regulates replication, ATM is the key mediator of the cellular response to DSBs. DNA-PK is the third member of this kinase family, however its functions are confined to local repair processes (Meek et al., 2008).

Phosphorylation, however, must act in concert with other PTMs, such as ubiquitylation, to elicit efficient responses to genotoxic insults (Ulrich and Walden, 2010). The functions of PTMs in the DNA damage and RS responses have therefore been subject of intense investigations, individually (Beli et al., 2012; Bennetzen et al., 2009; Danielsen et al., 2011; Jungmichel et al., 2013) and in concert (Gibbs-Seymour et al., 2015; González-Prieto et al., 2015; Hunter, 2007). More recently, studies have revealed the significance of protein SUMOylation in the DDR and deregulation of the SUMO system has been shown to confer genomic instability (Bergink and Jentsch, 2009; Bursomanno et al., 2015; Jackson and Durocher, 2013; Xiao et al., 2015). Using various RS inducing agents, these studies have shown that the SUMOylation status of a number of proteins is modulated when DNA replication is perturbed (García-Rodríguez et al., 2016). Furthermore, it has been demonstrated that phosphorylation and SUMOylation intersect at various levels (Gareau and Lima, 2010). A phosphorylation-dependent SUMO modification (PDSM) motif has been suggested to prime SUMOylation (Hietakangas et al., 2006) by enhancing the binding of the SUMO E2 enzyme UBC9 (Mohideen et al., 2009), and phosphorylation was also found to regulate the function of SUMO interacting motifs (SIMs) (Stehmeier and Muller, 2009). However, a potential global coordination of the SUMOylation response and the well-known phosphorylation response to RS remains unexplored.

Quantitative mass spectrometry (MS)-based proteomics and developments in enrichment methodologies have seen tremendous developments in recent years (Hendriks and Vertegaal, 2016). State-of-the-art MS technologies allow for the identification of thousands of SUMOylation sites (Hendriks et al., 2017; Lamoliatte et al., 2014, 2017; Schimmel et al., 2014; Tammsalu et al., 2014), and tens of thousands of phosphorylation sites from cellular systems (Francavilla et al., 2017; Mertins et al., 2016; Olsen et al., 2010). In this study, we utilized complementary proteomics strategies to identify the interplay between the global SUMOylation and phosphorylation responses to replication stressors. We identified regulation of thousands of phosphorylation sites and hundreds of SUMOylation sites in response to treatment with the DNA inter-strand crosslinking (ICL) agent mitomycin C (MMC) and to hydroxyurea (HU), with a number of proteins co-regulated by both PTMs. Our investigations revealed that the well-established apical responders to RS and RS induced DSBs, namely ATR and ATM, both modulate protein SUMOylation at various stages of the RS response. Our findings not only identify an intersection between phosphorylation and SUMOylation in the RS response, but also reveal further levels of signaling regulation in this response by the two most prominent kinases of the DNA damage and RS responses.

2 Results

2.1 Global SUMOylation changes upon MMC treatment

To investigate the interplay between the SUMOylation and phosphorylation responses to RS, we treated U-2-OS osteosarcoma cells with MMC (Figure 1A). MMC, a widely-used chemotherapeutic agent in treatment of various cancers, induces ICLs, thereby impeding normal replication fork progression and causing RS. To study the effects of MMC during DNA replication, cells were synchronized at the G1/S checkpoint by 24 hours of thymidine blocking, and were thereafter released into S-phase with or without MMC for 8 hours (Figure 1B, Figure S1A). After an 8 hours release into MMC, western blotting confirmed increased phosphorylation of checkpoint kinases, CHK1 at S435 and CHK2 at T68, as well as increased levels of phosphorylation of S140 on histone H2A.X (γH2AX) (Figure S1B). These phosphorylation sites are known targets of ATR and ATM indicating that our experimental conditions generate RS (ATR activation) and DSBs (ATM activation).

For MS based global analysis of SUMOylation we used two previously described SUMO-enrichment approaches to quantify changes in protein SUMOylation and SUMO acceptor sites (Hendriks et al., 2014; Schimmel et al., 2014) on a global scale (Figure 1B). SUMOylated proteins were identified and quantified by immuno-precipitation (IP) of SUMO2-conjugated proteins from U-2-OS cells stably expressing FLAG-SUMO2-Q87R (Figure 1C and Figure S1C). The Q87R mutation allows for identification of SUMO after tryptic digestion due to the resulting remnant (Schimmel et al., 2014). To confidently distinguish SUMOylated from non-SUMOylated proteins, control IPs were also performed from the parental U-2-OS cell line, as non-SUMOylated proteins would be underrepresented

in these compared to FLAG-SUMO-Q87R expressing cells (Figure 1B). Complementarily, we mapped SUMOylation acceptor sites by enrichment of SUMOylated peptides from His10-tagged SUMO2-K0-Q87R expressing U-2-OS cells (Figure 1B) (Xiao et al., 2015). Tryptic peptides from all enriched samples were analyzed by nano-scale liquid chromatography tandem MS (LC-MS/MS) on a Q-Exactive HF instrument (Kelstrup et al., 2014). We used stable isotope labeling by amino acids in cell culture (SILAC) (Ong, 2002) for accurate MS-based quantification and differentially labeled SILAC cells showed comparable cell-cycle distributions upon synchronization (Figure S1A). The SUMO2 expression levels in the two stable cell lines were 3 to 4 fold higher than in the parental cells as observed by MS full scans from proteome measurements and by western blotting (Figures S1D and S1E).

All raw LC-MS/MS files were processed and analyzed together using the MaxQuant software suite (www.maxquant.org) with one percent false discovery rate at peptide, site and protein levels (Cox and Mann, 2008). From this analysis, we confidently identified 3,453 proteins (Table S1). Ratios from proteome measurements of these conditions revealed that the protein abundances in the MMC treated FLAG-SUMO2-Q87R cells were largely unchanged compared to the equivalently treated parental cells. We therefore reasoned that we could determine the proteins significantly SUMOylated in the FLAG-SUMO2-Q87R cells using ratio cutoffs of two standard deviations from the mean (95^{th} percentile) of this ratio distribution (Figure S1F). This analysis resulted in a cutoff of 1.7 fold change, by which 702 proteins were deemed SUMOylated (Figure 1D and Table S1). Using the same strategy for the MMC treated and untreated FLAG-SUMO2-Q87R cells, a resulting ratio cutoff of 1.5 resulted in 187 proteins being having significantly increased SUMOylation upon treatment with MMC (Figures 1D, S1G and Table S1). Additionally, we mapped 311 unique SUMO acceptor sites (Figure 1E). Sequence motif analysis of these showed a strong preference for a glutamate two residues downstream from the modified lysine (Figure 1E), conforming to the previously described SUMOylation consensus motif (ΨKXE) (Sampson et al., 2001). By separately analyzing SUMOylated peptides with or without this motif, we found that indeed the known SUMO consensus motif is the predominant, with the inversed SUMO motif as the second most overrepresented (Figure 1E).

To determine the cellular compartments and biological processes in which the SUMOylated proteins are involved, we performed a Gene Ontology (GO) enrichment analysis. In agreement with previous studies, we found that the majority of SUMOylation occurs on nuclear proteins that are involved in transcription (Figure S1H) (Flotho and Melchior, 2013). Further to this, among the proteins with MMC regulated SUMOylation, we identified 24 transcription factors, for which 24 target genes were found to be co-regulated by at least two of these. Interestingly, these target genes were highly enriched in proteins involved in apoptosis and cancer development (Table S1). GO analysis of the 187 proteins with increased SUMOylation after MMC treatment also revealed this trend, and furthermore these proteins are involved in histone ubiquitylation and DNA repair (Figure 1F).

Many of the identified proteins known to function in DNA repair clustered together in a functional network based on STRING database analysis (Szklarczyk et al., 2015). Fanconi anemia factors, BRCA1

(Breast cancer type 1 susceptibility protein) and TOPBP1 (DNA topoisomerase 2-binding protein 1) were among the regulated SUMOylated proteins after MMC treatment (Figure 1G). These proteins are well-known to play important roles in response to ICL-induced RS and DNA damage. The regulation of SUMOylation levels on these proteins upon MMC treatment indicates that this modification may modulate their function in this response.

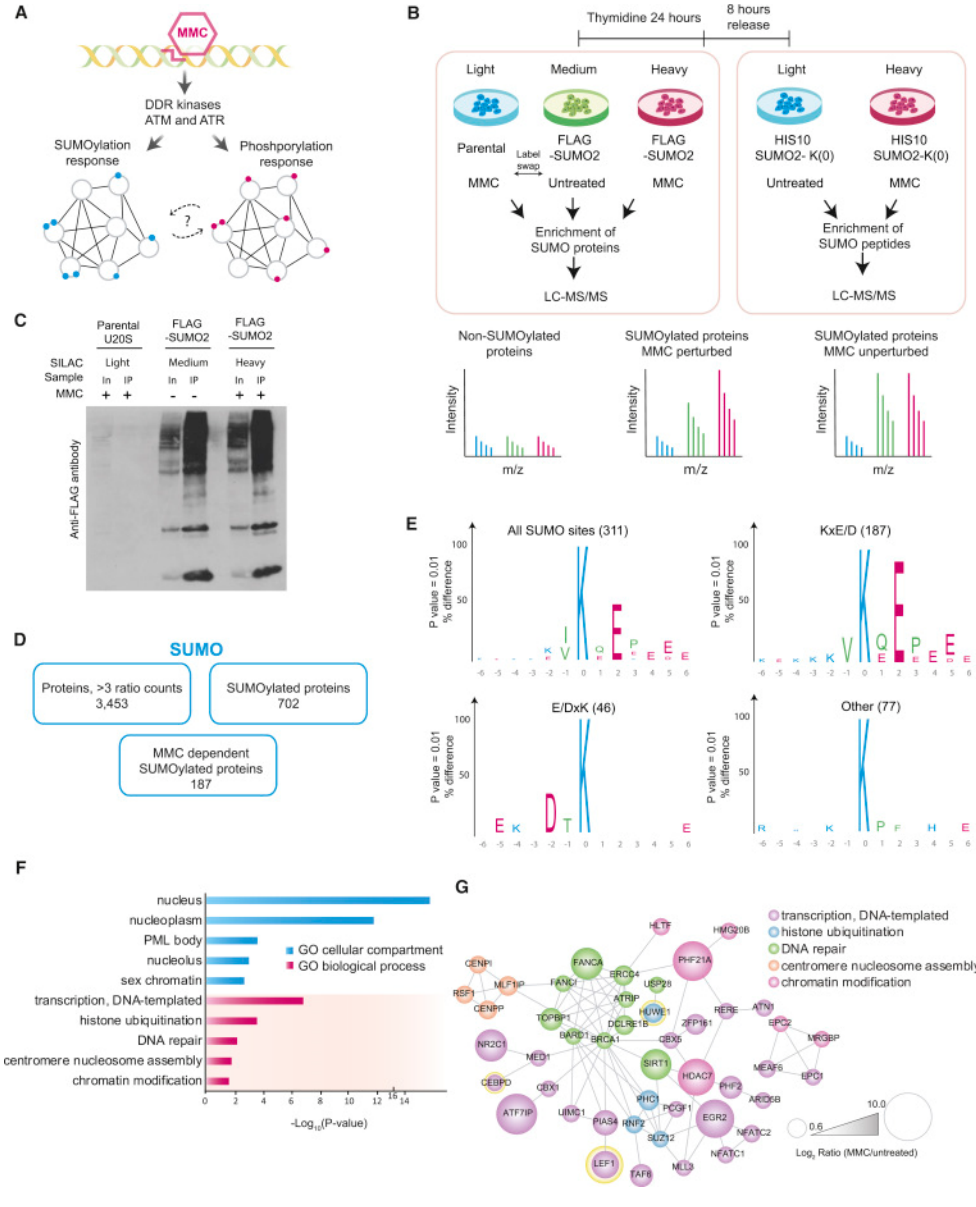

Figure 1 Proteomics analysis of SUMOylation changes upon MMC treatment. A) Schematic representation of the aim to study a potential interplay between phosphorylation and SUMOylation in MMC induced RS. **B)** Experimental design for proteomics analysis of SUMOylated proteins from FLAG-SUMO2 and His10-SUMO2 expressing U-2-OS cells to enrich SUMOylated proteins and peptides respectively. **C)** Western blot analysis of SUMO enriched proteins from SILAC labeled U-2-OS cells stably transfected with FLAG-SUMO2. Cells were synchronized and treated as in (A). **D)** Results of proteomics analysis. **E)** Motif analysis of SUMOylation acceptor sites. **F)** Enrichment analysis of GO cellular compartments (GOCC) and biological processes (GOBP) of MMC regulated SUMOylated proteins, using InnateDB**. G)** Functional network analysis of proteins from the GOBP terms enriched in (F). (See also Figure S1 and Table S1).

2.2 Global phosphorylation changes upon MMC treatment

To study the potential interplay between the SUMOylation and phosphorylation responses to MMC, we used a streamlined quantitative phosphoproteomics workflow (Batth et al., 2014) to enrich phospho-peptides from FLAG-SUMO2-Q87R U-2OS cells synchronized and treated with MMC in the same manner as for SUMOylation mapping. Tryptic digests of whole cell lysates were separated by offline high pH reversed-phase fractionation and phospho-peptides were enriched with TiO_2 beads prior to LC-MS/MS (Figure S2A). We quantified 20,900 high confidence phosphorylated sites, of which 650 were induced (SILAC ratio above 1.5) after 8 hours of MMC treatment (Figure 2A and Table S2). Proteins with induced phosphorylation were primarily nuclear and involved in DNA repair as determined by GO analysis, similar to our findings for SUMOylated proteins that were induced by MMC treatment (Figure 2B and S2B).

We performed sequence motif analysis of the 650 up-regulated phosphorylation sites to identify protein kinases that were activated in the response to MMC treatment. A strong overrepresentation of glutamine (Q) at the position directly C-terminal to the phosphorylation sites (P+1) indicated activation of the ATM and ATR kinases, both of which are known to preferentially phosphorylate substrates on serine/threonine residues that are followed by a glutamine (S/T-Q) (Figure 2C). Indeed, we find that 170 (26%) of the phosphorylation sites up-regulated by MMC treatment confer to the S/T-Q motif. Moreover, MS spectra show a clear induction of ATM and ATR target phosphorylation sites on ATM itself and CHK1, respectively (Figure 2D). Conversely, phosphorylation sites on proteins from other signaling pathways, as exemplified by ERK1, remained largely unperturbed (Figure 2D). Functional network analysis of the proteins with increased phosphorylation reveals two highly interconnected clusters of phosphoproteins involved in the DDR, DNA replication and cell cycle (Figure 2E). A number of these proteins were also found to have increased SUMOylation, indicating that phosphorylation and SUMOylation are modulating proteins in the same pathways in the RS response to MMC treatment.

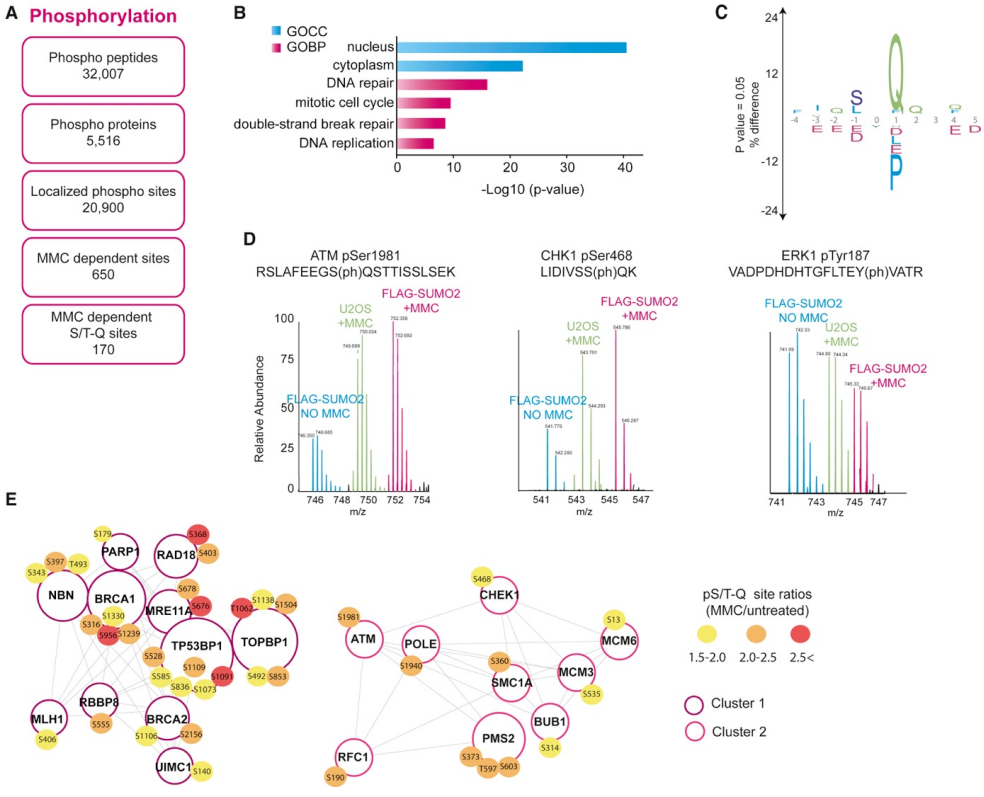

Figure 2 Phosphoproteomics analysis of MMC treated cells. A) Overview of number of phosphorylated peptides and proteins from phosphoproteomics analysis of cells treated as shown in Figure S2A. **B)** GOCC and GOBP analysis of proteins with regulated phosphorylation sites after MMC treatment, using InnateDB. **C)** Motif enrichment analysis of 360 MMC dependent phosphorylation sites, done with IceLogo**. D)** Full MS spectra of phosphorylated peptides from ATM, CHK1 and ERK1. **E)** Two highly interconnected MCODE clusters from functional network analysis of all proteins with regulated phosphorylation sites. MCODE was set to determine clusters with the 'Haircut' approach, a minimum node score cutoff of 0.2, K-core was set to 2 and max depth to 100. (See also Figure S2 and Table S2).

2.3 Central DDR proteins are highly phosphorylated and SUMOylated in the response to MMC

To elaborate on this hypothesis and uncover a potential interplay between the SUMOylation and phosphorylation responses to MMC, we integrated our large-scale proteomics datasets of the two modifications. First, we evaluated the datasets for potential biases arising from the MS strategies used for enrichment and detection of proteins with these modifications. The distribution of the relative protein copy numbers (iBAQ values) from the proteome, the phosphorylated proteins and the SUMOylated proteins in these datasets revealed that all three groups of proteins had similar distribution patterns with no apparent abundance biases (Figure S3A). We then assessed the overlap between the

datasets and found that 540 proteins harbored at least one SUMOylation and phosphorylation event (Figure 3A). This comprises two-thirds of the SUMOylated proteins we identified, corresponding to the proportion of the total proteome that is reported to be phosphorylated at any given time (Olsen et al., 2010). While only 17 of these proteins were found to have up-regulation of both modifications upon MMC treatment, this subset included UIMC1 (BRCA1-A complex subunit RAP80), BRCA1, BARD1 (BRCA1-associated RING domain protein 1), and TOPBP1, which are proteins with well-established key functions in the DDR (Figure 3A, 3B and Table S3). We therefore find that quantitative analysis of proteins co-regulated by both PTMs is powerful means to determine and prioritize key players in cellular signaling networks.

To elaborate on the mechanism of regulation of these two PTMs in RS, we further investigated the roles of most prominent DDR and RS activated kinases, namely ATR and ATM, in modulating RS induced SUMOylation (Smith et al., 2010). These kinases are the well-known initiators and key modulators of the global phosphorylation and ubiquitylation responses to DNA damage and RS (Shiloh, 2001). Indeed, ATR is activated upon 8 hours of MMC treatment after thymidine release, as observed by increased phosphorylation of its direct target CHK1 on S345, which can further be attenuated with an ATR inhibitor (ATRi) (Figure S3B). Interestingly, TOPBP1, an important co-activator of ATR, was the highest co-modified protein upon MMC treatment (Figure 3B). By SUMO enrichment from both the FLAG-SUMO2-Q87R and His10-tagged SUMO2-K0-Q87R cells, we were able to confirm that indeed TOPBP1 SUMOylation is increased over time with MMC treatment (Figure 3C). Since the His10-based pull-down procedures involved lysis and enrichment under harsh denaturing conditions, these findings confidently demonstrate that TOPBP1 is indeed differentially SUMOylated by RS and that the observed changes are not due to TOPBP1 interactions with other SUMO-regulated target proteins. Interestingly, TOPBP1 SUMOylation was further induced upon co-treatment of MMC with ATRi, also at earlier time points (Figure 3D). Although TOPBP1 SUMOylation is increased upon treatment with MMC or ATRi only, the combination of the two is required for massive hyper-SUMOylation (Figure 3D). ATM is also activated in these conditions as indicated by increased CHK2 and H2A.X phosphorylation (Figure 3D and S3B), and interestingly the hyper-SUMOylation of TOPBP1 upon MMC and ATRi co-treatment was significantly reduced by ATM inhibition (Figure 3D). Thus, in contrast to well-known phospho-induced SUMOylation, it appears that modulation of phosphorylation networks can also reduce SUMOylation in this context, expanding the repertoire of phospho-SUMO crosstalk.

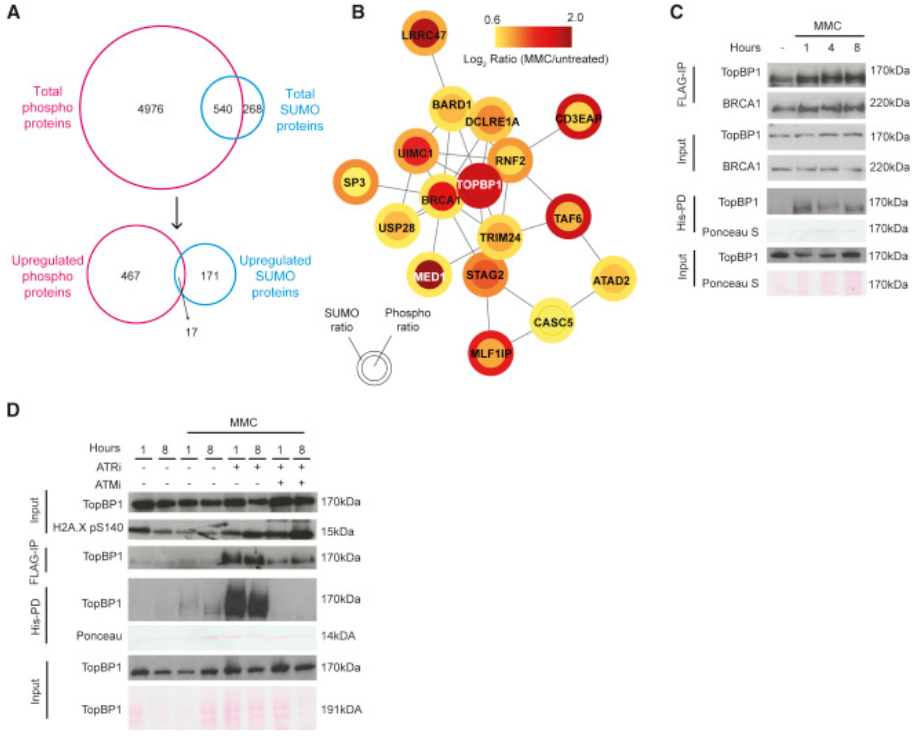

Figure 3 Integrated analyses of SUMOylation and phosphorylation datasets. A) Overlap of all identified and regulated SUMOylation and phosphorylation substrates. **B)** Functional network analysis of the 17 proteins with regulated phosphorylation and SUMOylation. **C)** Validation of TOPBP1 and BRCA1 regulated SUMOylation in FLAG-SUMO2 U-2-OS cells blocked for 24 hours with thymidine and then treated for 8 hour with or without MMC. Flag-IP: FLAG-based immuno-precipitation; His-PD: His-based pull down. **D)** Western blot analysis of TOPBP1 SUMOylation upon treatment with 8 hours MMC with and without ATR (ATRi, ATR-45) and ATM inhibitors (ATMi, KU55933). (See also Figure S3 and Table S3).

These observations are in accordance with induction of DNA DSBs and ATM activation that arises upon RS in combination with checkpoint inhibition (Toledo et al., 2013) (Figure 4A). To validate our observations that central DDR kinases modulate hyper-SUMOylation of TOPBP1 upon MMC treatment and determine whether such regulation occurs on other proteins, we performed an additional label-free quantitative proteomics screen. Here we analyzed enriched SUMOylated proteins from MMC treated cells in combination with the ATMi and ATRi (Figure 4B, Figure S4A and Table S4). We confirmed that TOPBP1 is hyper-SUMOylated by co-treatment with MMC and ATRi, and that this was attenuated upon addition of ATMi (Figure 4C and 4D). Remarkably, ATR itself, and its constitutive interactor ATRIP, which localizes ATR to TOPBP1 for activation, both displayed the same hyper-SUMOylation pattern as TOPBP1 (Figure 4C and 4D). While SUMOylation of ATRIP and ATR has previously been reported in response to UV and HU treatments (Wu et al., 2014), we find that hyper-

SUMOylation of ATR, ATRIP, TOPBP1, and XRCC6 (X-ray repair cross-complementing protein 6) arises upon RS in combination with checkpoint inhibition. Importantly, STRING-based functional network analysis of SUMOylation targets significantly regulated upon MMC treatment with and without ATRi and ATMi, reveals that these consist of core ATR activating proteins and DDR responders, showing remarkable orchestration of this functional group (Figure S4B) (Jentsch and Psakhye, 2013).

Together, these proteomics experiments suggest that regulation of phosphorylation and SUMOylation occurs within overlapping networks of RS responders, and that these may be subjected to common control by the same apical DDR kinases.

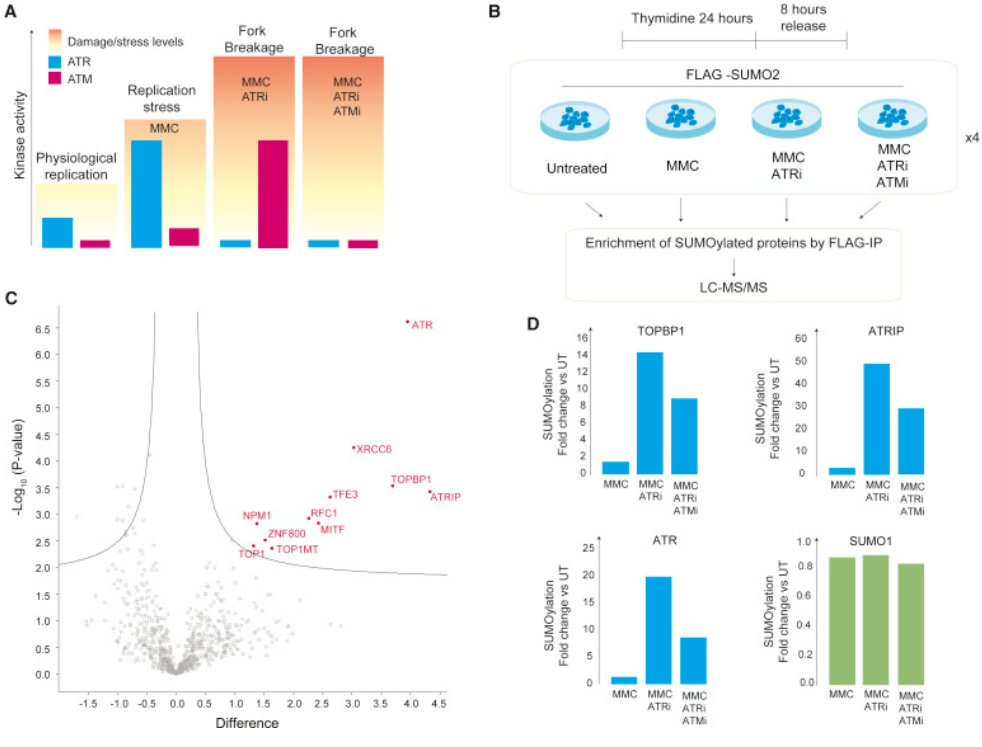

Figure 4 Proteomics analysis of TOPBP1 SUMOylation regulation by ATR and ATM inhibitors. A) Schematic representation of kinase activities at progressive stages of RS induced by MMC treatment and in combination with ATR and ATM inhibition. The blue and red bars represent the level of activation of the ATR and ATM kinases respectively. The shaded backgrounds represent the increasing levels of replication stress and damage that can be induced by MMC and ATRi co-treatment, yellow being less and red being extreme RS. **B)** Experimental design for label-free proteomics analysis of TOPBP1 SUMOylation upon MMC treatment with and without ATRi (ATR-45) and ATMi (KU55933), in FLAG-SUMO2 U-2-OS cells. **C)** Volcano plot of all ratios of MMC and ATR treated cells compared to MMC alone from enriched SUMOylated proteins, using t-test to determine significantly modulated (FDR<0.05) targets (indicated in red). C) SUMOylation levels for

TOPBP1, ATR and ATRIP from the proteomics analysis, and SUMO as a negative control. UT: untreated (cells that were released into DMSO without MMC or inhibitors) (See also Figure S4 and Table S4).

2.4 ATM and ATR modulate a global SUMOylation response to RS

We next sought to determine whether modulation of protein SUMOylation by ATM and ATR was a general mechanism in other conditions of RS. Using (HU), an inhibitor of dNTP synthesis, which causes DNA replication fork stalling, we could reproduce the pattern of TOPBP1 SUMOylation observed for MMC with and without ATRi and ATMi co-treatment (Figure 5A). TOPBP1 SUMOylation was increased upon 3 hours of HU treatment, further massively enhanced by co-treatment with ATRi, and then attenuated by addition of ATMi (Figure 5A). However, after 30 min HU and ATRi treatment, only modest increase of TOPBP1 SUMOylation was detected. This pattern is in accordance with replication forks breaking after longer treatments with replication stressors and checkpoint inhibition, thereby also inducing ATM signaling (Figure 5A and Figure S5A). Furthermore, treatment with high-dose ionizing radiation (IR), which also induces DSBs and ATM activation, did not induce TOPBP1 SUMOylation, indicating that this regulation is specific to RS associated DNA breaks (Figure 5A). We further validated this pattern of TOPBP1 SUMOylation using two different pharmacological inhibitors for ATM and ATR and with one CHK1 inhibitor (CHK1i) (Figure S5A). Analogous to ATR, inhibition of CHK1, a prominent substrate and mediator of ATR checkpoint signaling, results in replication fork breakage and ATM activation (Figure S5A). Interestingly, TOPBP1 was also hyper-SUMOylated upon CHK1i and HU co-treatment (Figure S5A). Collectively, these observations indicate that modulation of the SUMOylation response to RS by these central DDR kinase could be a general regulatory mechanism, and not only specific to MMC treatment.

To elaborate on the magnitude of this mechanism, we performed a large-scale proteomics experiment to analyze SUMOylation and phosphorylation site regulation under these conditions. Specifically, we enriched SUMOylated and phosphorylated peptides from cells treated with HU in combinations with and without CHK1i and ATMi for analysis by LC-MS/MS (Figure S5B and S5C). CHKi was used rather than ATRi to permit initiation of the RS response by ATR. Four biological replicates were performed and each sample was analyzed twice by MS for label free quantification (Figure S5D). We identified 3,465 SUMOylated peptides corresponding to 1,590 SUMOylation acceptor sites, of which 2,450 peptides were quantified at least three times in at least one of the three treatment conditions (Figure 5B and Table S5). Using ANOVA significance testing to compare the dynamics of the modifications between treatments, 1,374 SUMOylated peptides, corresponding to 816 SUMO acceptor sites, were deemed regulated in at least one condition (Figure 5B). Similarly, 3,373 high confidence phosphorylation sites were found to be modulated and 127 proteins harbored changes of both PTMs (Figure 5B and 5C). To determine whether there was interdependency between SUMOylation and phosphorylation in our dataset, for example with the PDSM motif (Hietakangas et

al., 2006), we analyzed our raw MS data to identify co-occurring phosphorylation sites on the enriched SUMO peptides. We identified 127 phosphorylation sites in the SUMO-enriched dataset of which 26 were on SUMOylated peptides (Table S5). While the overlap is modest, 64% of these phosphorylation sites harbored a proline in the residue directly C-terminal to the phosphorylated serine/threonine residue, conforming to part of the PDSM motif (ΨKxExxSP) (Table S5).

We further analyzed our dataset to determine the degree of control that the DDR kinases exert on protein SUMOylation in response to RS. It is evident from the number of significantly perturbed SUMOylation acceptor sites, that regulation of this modification by ATM and ATR is a global mechanism in the response to RS, as more than fifty percent of the quantified sites were significantly regulated (Figure 5B). We performed unsupervised hierarchical clustering of the regulated phosphorylation sites and SUMOylated peptides to determine the dynamics of this regulation (Figures 5D and S5E). For both modifications we identified a cluster that showed the same dependency on CHK1 and ATM as observed for TOPBP1 by western blotting (Figure 5D). In this cluster, protein SUMOylation and phosphorylation sites increased upon co-treatment of HU with CHK1i compared to HU alone, and was attenuated upon further addition of ATMi (Figure 5D and S5E). Interestingly, GO analysis revealed that these clusters were enriched in proteins involved in DNA replication and recombination (Figure 5D and S5E). Among the SUMO-regulated proteins in this cluster were key regulators of DNA replication and homologous recombination such as TOP2A (DNA topoisomerase 2-alpha), BLM (Bloom syndrome protein), and BRCA1 as well as its constitutive interactor BARD1 (Figure 5D). Moreover, the dynamics of the modifications in these specific clusters are in accordance with the expected and observed phosphorylation profiles of targets of ATR and ATM (Figure 5A, 5D, S5A and S5E). Additionally, a cluster of proteins with significantly increased SUMOylation upon HU and CHK1i co-treatment, but unchanged by addition of ATMi, were enriched in proteins involved in DDR and DNA repair (Figure 5D). This included UIMC1, RBBP((CtIP), and interestingly also TOPORS, a SUMO E3 ligase that is known to play a role in the DDR (Lin et al., 2005; Marshall et al., 2010). Noteworthy, a substantial fraction of SUMOylation sites were modulated inversely, being unaffected or only slightly modulated by CHK1 inhibition, yet increasing dramatically upon co-inhibition of ATM (Figure 5D). This further indicates that ATM is a central regulator of protein SUMOylation in the DDR, and possibly more specifically in protein *de*SUMOylation. This subset of SUMO-regulated proteins was enriched for house-keeping biological processes such as RNA metabolism, transcription and chromatin remodeling (Figure 5D). Our findings demonstrate that SUMOylation is regulated globally in response to RS by the chief DDR kinases, ATM and ATR.

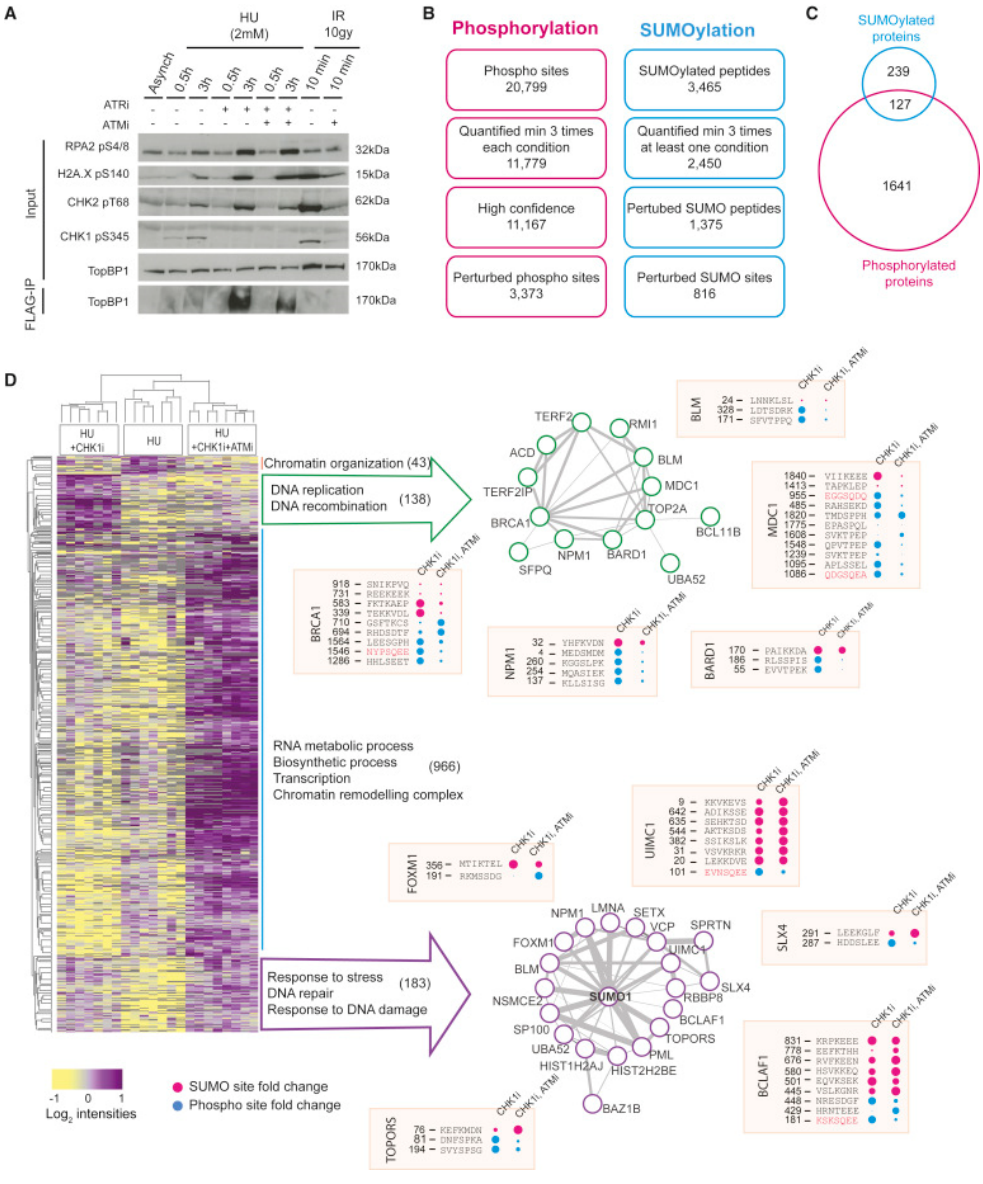

Figure 5 Deep proteomics analysis of phosphorylation and SUMOylation in RS and replication fork breakage. A) Western blot analysis of TOPBP1 SUMOylation and markers of ATR and ATM activity upon treatment with HU with and without ATRi (ATR-45) and/or ATMi (KU55933). **B)** Number of peptides, sites and proteins identified and quantified from the proteomics analysis. Total phosphorylation sites and SUMOylated peptides from all experimental conditions with a 1% FDR rate. Targets quantified at least three times from all biological and technical replicates in at least one condition were used for further analysis. For phosphorylation events, localization probabilities of at least 0.75 (high confidence) was also required. Perturbed SUMOylation peptides and phosphorylation sites that were modulated in any one condition compared to another were determined by ANOVA testing (FDR < 0.05). **C)** Overlap of proteins with regulated SUMOylation and phosphorylated.

D) Unsupervised hierarchical clustering of the 1,375 significantly perturbed SUMOylation. GOBP enrichment analysis of the clusters, with STRING-based functional network analysis of the proteins in the clusters and dotplot representation of SUMOylation and phosphorylation site changes on selected proteins (pink for SUMOylation sites and blue for phosphorylation sites). The modified sequence is with the modification site in the center, and the red phospho-peptide sequences are those that confer to the ATM and ATR sequence motif, S/T-Q. (See also Figure S5 and Table S5).

3 Discussion

Context-specific and dynamic post-translational protein modifications are well-established regulators of the signaling pathways that protect eukaryotic DNA integrity during the tremendous task of replication. Advancements in speed, resolution and sensitivity of MS-based technologies have revolutionized the study of global PTM biology (Olsen and Mann, 2013). With this rise in global PTM data, it has become evident that efficient cellular responses, such as those that safeguard genomic integrity, require the precise and timely coordination of several PTMs and the different enzymes that regulate them (Papouli et al., 2005). Integrated analysis of PTMs is therefore pertinent for our understanding of the molecular mechanisms that respond to DNA damage and RS. Using state-of-the-art proteomics methodologies, we mapped nearly 1,400 regulated SUMOylation acceptor sites and 3,300 regulated phosphorylation sites, in response to the chemotherapeutic agents MMC and HU. Our study reveals that SUMOylation is regulated by the most dominant, apical DDR kinases, ATR and ATM, which are known to initiate and coordinate the phosphorylation responses to RS and replication fork breakage.

In accordance with previous studies, we find that RS elicits increased SUMOylation of the core ATR activating proteins, including TOPBP1 and ATRIP. Interestingly, previous studies have shown the SUMOylation of ATR and its constitutive interactor ATRIP are necessary for efficient ATR dependent checkpoint signaling (Wu and Zou, 2016; Wu et al., 2014). Further to this, here we showed that TOPBP1, a key co-activator of ATR, undergoes increased SUMOylation in response to MMC induced RS. This indicates that SUMOylation of this factor, in addition to that of ATR and ATRIP, may be important for ATR dependent checkpoint signaling. However, further biochemical and molecular biological analysis is required to confirm the precise role of TOPBP1 SUMOylation in ATR activation. In addition, our data suggest that SUMOylation is a common and relevant modification of a number of proteins involved in ATR activation in response to RS.

We aimed to uncover the interplay between phosphorylation and SUMOylation of protein networks in the RS response. Using an integrated proteomics approach, we found that protein SUMOylation was widely modulated by the main regulatory kinases that mediate the phosphorylation response. Parallel proteomics analysis of changes in these two PTMs revealed co-regulation of a number of central RS and DDR responders including BRCA1, BARD1 and TOPBP1. BRCA1 SUMOylation and phosphorylation have individually been found to play a key role in the function of this protein, as SUMOylation has been shown to increases its ubiquitin ligase activity (Morris et al., 2009). It will be

interesting in future analysis to determine whether there is co-dependency or cross regulation of these modifications in the proteins that harbor both phosphorylation and SUMOylation, and in particular the relevance of this for the functions of central DDR proteins.

Our approach, to study co-regulated SUMO- and phospho-modified proteins, proved successful to identify key co-modified targets. TOPBP1 was the most highly co-regulated protein in our dataset upon eight hours of MMC treatment, and we found that TOPBP1 SUMOylation was heavily modulated by ATR inhibition during RS and by ATM upon replication fork breakage. We found this particularly interesting, as these central DDR kinases (particularly ATM) are well known to orchestrate various PTM-based networks upon threats to the DNA (Smith et al., 2010). However, the effect of the apical DDR kinases on global protein SUMOylation in response to DNA damage and replication stress has not yet been shown. We determined that such regulation by kinases not only applies to TOPBP1, but further to nearly 1,400 SUMOylation acceptor sites in response to HU induced RS, demonstrating global regulation of SUMOylation by these kinases in the maintenance of genome stability. Interestingly, we observed decreased SUMOylation of a large subset of proteins upon ATM inhibition under conditions that induce replication fork breakage. This suggests that ATM may be important for global *de*SUMOylation to maintain and control physiological levels of protein SUMOylation.

In our bioinformatics analysis of proteins with increased SUMOylation upon treatment with MMC and HU, we found clusters of co-regulated proteins that are known to function together in the RS response. In addition to the ATR activation proteins, BRCA1 and BARD1, we also found Fanconi Anemia proteins and DSB response proteins like MDC1, NBN and CtIP. This is particularly interesting in light of the recent idea that SUMO functions as a molecular glue to mediate protein complex formation under specific cellular states, and that this modification takes form of a ‘SUMO-spray’ (Jentsch and Psakhye, 2013). A consequence of this hypothesis is that SUMOylation should occur on functionally related proteins, to promote cooperation and interaction in protein networks, and this is precisely what we observe in our dataset. Interestingly, we find that proteins co-modified by SUMOylation and phosphorylation, generally have many regulated sites in response to RS. This poses a challenge for functional studies as site-directed mutagenesis of specific SUMOylation acceptor sites has been shown to result in little effect on overall protein SUMOylation or function (Jentsch and Psakhye, 2013).

Here we present an integrated analysis of global protein phosphorylation and SUMOylation in RS responses, and the largest resource to date of regulated SUMOylation targets in these conditions. We propose that increased SUMOylation occurs on specific and relevant factors in response to distinct DNA lesions, as illustrated by the SUMOylation dynamics upon RS and RS induced DSBs. Our data suggests that these SUMOylation responses are orchestrated by the apical kinases ATR and ATM in parallel with or as part of their phosphorylation signaling. These findings and further investigations of the co-regulation of these two modifications, is currently of great interest, in that the induction of RS provoked DSBs is increasingly used in chemotherapy to induce cancer cell killing (Li and Heyer, 2008).

In light of the essential role of SUMO in maintenance of genomic integrity (Bergink and Jentsch, 2009; Jackson and Durocher, 2013), the increasing interest of this system as a druggable target (Kessler et al., 2012) will require the understanding of how its perturbation affects global signaling networks.

4 Experimental procedures

Further details and an outline of resources used in this work can be found in Supplemental Experimental Procedures.

4.1 Cell culture

Human U-2-OS osteosarcoma cells cultured in complete DMEM, and for SILAC based experiments cells were SILAC labeled as reported previously (Hekmat et al., 2013; Olsen et al., 2006. For further details on cell culture, synchronization and drug treatments see Supplemental experimental procedures.

4.2 Stable cell line generation

To generate stable cell lines for SUMO enrichment U-2-OS cells were infected with lentivrus encoding either FLAG-tagged SUMO-2 (FLAG-SUMO2) or His10-SUMO-2-K0-Q87R (His10-S2-K0) as previously described (Hendriks et al., 2014; Schimmel et al., 2014). Further details are provided in Supplemental experimental procedures.

4.3 SUMO target protein enrichment

Enrichment of SUMOylated proteins was performed as previously described (Schimmel et al., 2014). Briefly cell were harvested in lysis buffer and sonicated, prior to enrichment of SUMOylated protein using Monoclonal ANTI-FLAG M2 beads (Sigma) for 90min at 4ºC with rotation. Following washes, the bound proteins were eluted using 1mM FLAG-M2 epitope peptide and thereafter filtered through a Amicon Ultra 10k NMWL spin filter (Millipore). The resulting proteins were processed by in-gel digestion for LC-MS/MS analysis. For detail on enrichment of SUMO target proteins and in-gel digestion, please see Supplemental experimental procedures.

4.4 SUMO-peptide enrichment

SUMOylated peptides were enriched as previously described in (Hendriks et al., 2014). Briefly, thirty 15 cm plates of U-2-OS per condition were harvested in PBS, lysed in a 6M guanidine-HCl lysis buffer and sonicated. SUMOylated proteins were enriched from equal amounts of protein for each condition by Ni-NTA agarose beads overnight at 4ºC. Proteins were eluted using 500mM imidazole two times. The eluted proteins were filtered and concentrated in spin filters digested with LysC. SUMOylated peptides were subsequently enriched with Ni-NTA agarose beads at 4°C for 5 hours, and eluted using 500mM imidazole. The enriched peptides were filtered and concentrated prior to digestion with trypsin and analysis by LC-MS/MS. For detailed SUMO-peptide enrichment procedures see Supplemental experimental procedures.

4.5 Mass Spectrometry analysis

Peptide mixtures were analyzed using an EASY-nLC system (Proxeon, Odense, Denmark) connected to a Q-Exactive mass spectrometer (Thermo Fisher Scientific, Bremem, Germany), as described (Kelstrup et al., 2012). Details are provided in Supplemental experimental procedures.

4.6 Raw Data Processing

Raw data was analyzed using MaxQuant v1.4.1. and v1.5.11 against the complete human UniProt database. See Supplemental experimental procedures for detailed descriptions.

4.7 Bioinformatics analysis

All functional network analysis were done using the String database (Szklarczyk et al., 2015) and further processed with Cytoscape (www.cytoscape.org). Hierarchical clustering and ANOVA t-test were performed using Perseus. For ANOVA the FDR threshold was set to 0.05. Sequence motif analysis was performed using IceLogo (Colaert et al., 2009). Details are provided in Supplemental experimental procedures.

Author Contributions

J.O.S. performed experiments described in Figures 1-4. Z.X. performed experiments described in Figure 5. T.S.B provided help and performed part dataset presented in Figure 2. G.F did validation experiments presented in Figure S5. L.v.S. and A.J.L.C. supervised J.O.S and S.M. and gave critical input on manuscript. A.C.O.V. supervised Z.X., J.V.O supervised J.O.S., and S.M. generated and analyzed the data shown in remaining figures. S.M., A.C.O.V. and J.V.O. conceived the study, designed the experiments, critically evaluated the results, and wrote the manuscript.

Data and software availability

All raw mass spectrometric data files for this study have been deposited to the ProteomeXchange Consortium via with the dataset identifier PXD006361.

Acknowledgements

Work at The Novo Nordisk Foundation Center for Protein Research (CPR) is funded in part by a generous donation from the Novo Nordisk Foundation (Grant number NNF14CC0001). The proteomics technology developments applied was part of a project that has received funding from the European Union's Horizon 2020 research and innovation programme under grant agreement No 686547. We would like to thank the PRO-MS Danish National Mass Spectrometry Platform for Functional Proteomics and the CPR Mass Spectrometry Platform for instrument support and assistance. L.V.S work was supported by the Danish Research Council (research career program FSS Sapere Aude). J.V.O. was supported by the Danish Cancer Society (R90-A5844 KBVU project grant) and Lundbeckfonden (R191-2015-703). A.C.O.V. was supported by the European Research Council (310913) and by the Netherlands Organisation for Scientific Research (NWO 93511037). J.O.S, Z.X., A.C.O.V. and J.V.O. were supported by the Marie Curie Initial Training Networks program of the European Union (290257-UPStream). A.J.L and S. M. were supported by Danish Cancer Society (KBVU-2014) and European Research Council (ERC-2015-STG-294679068) grants. A.J.L. lab was also supported by the Danish National Research Foundation (DNRF115) and Danish Council for Independent Research (Sapere Aude, DFF-Starting Grant 2014).

References

Batth, T.S., Francavilla, C., and Olsen, J. V. (2014). Off-line high-pH reversed-phase fractionation for in-depth phosphoproteomics. J. Proteome Res.

Beli, P., Lukashchuk, N., Wagner, S.A., Weinert, B.T., Olsen, J. V, Baskcomb, L., Mann, M., Jackson, S.P., and Choudhary, C. (2012). Proteomic investigations reveal a role for RNA processing factor THRAP3 in the DNA damage response. Mol. Cell *46*, 212–225.

Bennetzen, M., Larsen, D.H., Bunkenborg, J., Bartek, J., Lukas, J., and Andersen, J.S. (2009). Site-specific phosphorylation dynamics of the nuclear proteome during the DNA damage response.

Bergink, S., and Jentsch, S. (2009). Principles of ubiquitin and SUMO modifications in DNA repair. Nature *458*, 461–467.

Bursomanno, S., Beli, P., Khan, A.M., Minocherhomji, S., Wagner, S.A., Bekker-Jensen, S., Mailand, N., Choudhary, C., Hickson, I.D., and Liu, Y. (2015). Proteome-wide analysis of SUMO2 targets in response to pathological DNA replication stress in human cells. DNA Repair (Amst). *25*, 84–96.

Colaert, N., Helsens, K., Martens, L., Vandekerckhove, J., and Gevaert, K. (2009). Improved visualization of protein consensus sequences by iceLogo. Nat. Methods *6*, 786–787.

Cox, J., and Mann, M. (2008). MaxQuant enables high peptide identification rates, individualized p.p.b.-range mass accuracies and proteome-wide protein quantification. Nat. Biotechnol. *26*, 1367–1372.

Danielsen, J.M.R., Sylvestersen, K.B., Bekker-Jensen, S., Szklarczyk, D., Poulsen, J.W., Horn, H., Jensen, L.J., Mailand, N., and Nielsen, M.L. (2011). Mass spectrometric analysis of lysine ubiquitylation reveals promiscuity at site level. Mol. Cell. Proteomics *10*, M110.003590.

Flotho, A., and Melchior, F. (2013). Sumoylation: A Regulatory Protein Modification in Health and Disease. Annu. Rev. Biochem. *82*, 357–385.

Francavilla, C., Lupia, M., Tsafou, K., Villa, A., Kowalczyk, K., Rakownikow Jersie-Christensen, R., Bertalot, G., Confalonieri, S., Brunak, S., Jensen, L.J., et al. (2017). Phosphoproteomics of Primary Cells Reveals Druggable Kinase Signatures in Ovarian Cancer. Cell Rep. *18*, 3242–3256.

García-Rodríguez, N., Wong, R.P., and Ulrich, H.D. (2016). Functions of Ubiquitin and SUMO in DNA Replication and Replication Stress. Front. Genet. *7*, 87.

Gareau, J.R., and Lima, C.D. (2010). The SUMO pathway: emerging mechanisms that shape specificity, conjugation and recognition. Nat. Publ. Gr. *11*.

Gibbs-Seymour, I., Oka, Y., Rajendra, E., Weinert, B.T., Passmore, L.A., Patel, K.J., Olsen, J. V, Choudhary, C., Bekker-Jensen, S., and Mailand, N. (2015). Ubiquitin-SUMO Circuitry Controls Activated Fanconi Anemia ID Complex Dosage in Response to DNA Damage. Mol. Cell *57*, 150–164.

González-Prieto, R., Cuijpers, S.A., Luijsterburg, M.S., van Attikum, H., and Vertegaal, A.C. (2015). SUMOylation and PARylation cooperate to recruit and stabilize SLX4 at DNA damage sites. EMBO Rep. e201440017.

Halazonetis, T.D., Gorgoulis, V.G., and Bartek, J. (2008). An Oncogene-Induced DNA Damage Model for Cancer Development. Science (80-.). *319*.

Hendriks, I.A., and Vertegaal, A.C.O. (2016). A comprehensive compilation of SUMO proteomics. Nat. Rev. Mol. Cell Biol. *17*, 581–595.

Hendriks, I.A., D'Souza, R.C., Yang, B., Verlaan-de Vries, M., Mann, M., and Vertegaal, A.C. (2014). Uncovering global SUMOylation signaling networks in a site-specific manner. Nat Struct Mol Biol *21*, 927–936.

Hendriks, I.A., Lyon, D., Young, C., Jensen, L.J., Vertegaal, A.C.O., and Nielsen, M.L. (2017). Site-specific mapping of the human SUMO proteome reveals co-modification with phosphorylation. Nat. Struct. Mol. Biol. *24*, 325–336.

Hietakangas, V., Anckar, J., Blomster, H.A., Fujimoto, M., Palvimo, J.J., Nakai, A., Sistonen, L., and Walter, P. (2006). PDSM, a motif for phosphorylation-dependent SUMO modification.

Hunter, T. (2007). The age of crosstalk: phosphorylation, ubiquitination, and beyond. Mol. Cell *28*, 730–738.

Jackson, S.P., and Bartek, J. (2009). The DNA-damage response in human biology and disease. Nature *461*.

Jackson, S.P., and Durocher, D. (2013). Regulation of DNA Damage Responses by Ubiquitin and SUMO. Mol. Cell *49*, 795–807.

Jentsch, S., and Psakhye, I. (2013). Control of Nuclear Activities by Substrate-Selective and Protein-Group SUMOylation. Annu. Rev. Genet *47*, 167–186.

Jungmichel, S., Rosenthal, F., Altmeyer, M., Lukas, J., Hottiger, M.O., and Nielsen, M.L. (2013). Proteome-wide identification of poly(ADP-Ribosyl)ation targets in different genotoxic stress responses. Mol. Cell *52*, 272–285.

Kelstrup, C.D., Young, C., Lavallee, R., Nielsen, M.L., and Olsen, J. V. (2012). Optimized Fast and Sensitive Acquisition Methods for Shotgun Proteomics on a Quadrupole Orbitrap Mass Spectrometer. J. Proteome Res. *11*, 3487–3497.

Kelstrup, C.D., Jersie-Christensen, R.R., Batth, T.S., Arrey, T.N., Kuehn, A., Kellmann, M., and Olsen, J. V (2014). Rapid and deep proteomes by faster sequencing on a benchtop quadrupole ultra-high-field orbitrap mass spectrometer. J. Proteome Res. *13*, 6187–6195.

Kessler, J.D., Kahle, K.T., Sun, T., Meerbrey, K.L., Schlabach, M.R., Schmitt, E.M., Skinner, S.O., Xu, Q., Li, M.Z., Hartman, Z.C., et al. (2012). A SUMOylation-Dependent Transcriptional Subprogram Is Required for Myc-Driven Tumorigenesis. Science (80-.). *335*.

Kim, S.-T., Lim, D.-S., Canman, C.E., and Kastan, M.B. (2009). Substrate Specificities and Identification of Putative Substrates of ATM Kinase Family Members*.

Lamoliatte, F., Caron, D., Durette, C., Mahrouche, L., Maroui, M.A., Caron-Lizotte, O., Bonneil, E., Chelbi-Alix, M.K., and Thibault, P. (2014). Large-scale analysis of lysine SUMOylation by SUMO remnant immunoaffinity profiling. Nat. Commun. *5*, 5409.

Lamoliatte, F., McManus, F.P., Maarifi, G., Chelbi-Alix, M.K., and Thibault, P. (2017). Uncovering the SUMOylation and ubiquitylation crosstalk in human cells using sequential peptide immunopurification. Nat. Commun. *8*, 14109.

Li, X., and Heyer, W.-D. (2008). Homologous recombination in DNA repair and DNA damage tolerance. Cell Res. *181*.

Lin, L., Ozaki, T., Takada, Y., Kageyama, H., Nakamura, Y., Hata, A., Zhang, J.-H., Simonds, W.F., Nakagawara, A., and Koseki, H. (2005). topors, a p53 and topoisomerase I-binding RING finger protein, is a coactivator of p53 in growth suppression induced by DNA damage. Oncogene *24*, 3385–3396.

López-Contreras, A.J., and Fernandez-Capetillo, O. (2010). The ATR barrier to replication-born DNA damage. DNA Repair (Amst). *9*, 1249–1255.

Marshall, H., Bhaumik, M., Aviv, H., Moore, D., Yao, M., Dutta, J., Rahim, H., Gounder, M., Ganesan, S., Saleem, A., et al. (2010). Deficiency of the dual ubiquitin/SUMO ligase Topors results in genetic instability and an increased rate of malignancy in mice. BMC Mol. Biol. *11*.

Meek, K., Dang, V., and Lees-Miller, S.P. (2008). Chapter 2 DNA-PK: The Means to Justify the Ends? Adv. Immunol. *99*, 33–58.

Mertins, P., Mani, D.R., Ruggles, K. V, Gillette, M.A., Clauser, K.R., Wang, P., Wang, X., Qiao, J.W., Cao, S., Petralia, F., et al. (2016). Proteogenomics connects somatic mutations to signalling in breast cancer. Nature *534*, 55–62.

Mohideen, F., Capili, A.D., Bilimoria, P.M., Yamada, T., Bonni, A., and Lima, C.D. (2009). A molecular basis for phosphorylation-dependent SUMO conjugation by the E2 UBC9. Nat. Struct. Mol. Biol. *16*.

Morris, J.R., Boutell, C., Keppler, M., Densham, R., Weekes, D., Alamshah, A., Butler, L., Galanty, Y., Pangon, L., Kiuchi, T., et al. (2009). The SUMO modification pathway is involved in the BRCA1 response to genotoxic stress. Nature *462*.

Murga, M., Bunting, S., Montaña, M.F., Soria, R., Mulero, F., Cañamero, M., Lee, Y., Mckinnon, P.J., Nussenzweig, A., and Fernandez-Capetillo, O. (2009). A mouse model of ATR-Seckel shows embryonic replicative stress and accelerated aging. Nat. Publ. Gr. *41*.

Olsen, J. V, and Mann, M. (2013). Status of large-scale analysis of post-translational modifications by mass spectrometry. Mol. Cell. Proteomics *12*, 3444–3452.

Olsen, J. V., Vermeulen, M., Santamaria, A., Kumar, C., Miller, M.L., Jensen, L.J., Gnad, F., Cox, J., Jensen, T.S., Nigg, E.A., et al. (2010). Quantitative Phosphoproteomics Reveals Widespread Full Phosphorylation Site Occupancy During Mitosis. Sci. Signal. *3*.

Ong, S.-E. (2002). Stable Isotope Labeling by Amino Acids in Cell Culture, SILAC, as a Simple and Accurate Approach to Expression Proteomics. Mol. Cell. Proteomics *1*, 376–386.

Papouli, E., Chen, S., Davies, A.A., Huttner, D., Krejci, L., Sung, P., and Ulrich, H.D. (2005). Crosstalk between SUMO and Ubiquitin on PCNA Is Mediated by Recruitment of the Helicase Srs2p monoubiquitination serves alternative functions (Hicke, 2001), and depending on the linkage between the ubiq- uitin moieties, polyubiquitin chains can also convey. Mol. Cell *19*, 123–133.

Polo, S., and Jackson, S. (2011). Dynamics of DNA damage response proteins at DNA breaks: a focus on protein modifications. Genes Dev. *25*, 409–433.

Sampson, D. a., Wang, M., and Matunis, M.J. (2001). The Small Ubiquitin-like Modifier-1 (SUMO-1) Consensus Sequence Mediates Ubc9 Binding and is Essential for SUMO-1 Modification. J. Biol. Chem. *276*, 21664–21669.

Schimmel, J., Eifler, K., Otti Sigurðsson, J., Cuijpers, S.A., Hendriks, I.A., Verlaan-de Vries, M., Kelstrup, C.D., Francavilla, C., Medema, R.H., Olsen, J. V, et al. (2014). Molecular Cell Resource Uncovering SUMOylation Dynamics during Cell-Cycle Progression Reveals FoxM1 as a Key Mitotic SUMO Target Protein. Mol. Cell *53*, 1053–1066.

Shiloh, Y. (2001). ATM and ATR: networking cellular responses to DNA damage. Curr. Opin. Genet. Dev. *11*, 71–77.

Smith, J., Tho, L.M., Xu, N., and Gillespie, D.A. (2010). Chapter 3 - The ATM-Chk2 and ATR-Chk1 Pathways

in DNA Damage Signaling and Cancer. Adv. Cancer Res. *108*, 73–112.
Stehmeier, P., and Muller, S. (2009). Phospho-Regulated SUMO Interaction Modules Connect the SUMO System to CK2 Signaling. Mol. Cell *33*, 400–409.
Szklarczyk, D., Franceschini, A., Wyder, S., Forslund, K., Heller, D., Huerta-Cepas, J., Simonovic, M., Roth, A., Santos, A., Tsafou, K.P., et al. (2015). STRING v10: protein-protein interaction networks, integrated over the tree of life. Nucleic Acids Res. *43*, D447-52.
Tammsalu, T., Matic, I., Jaffray, E.G., Ibrahim, A.F.M., Tatham, M.H., and Hay, R.T. (2014). Proteome-Wide Identification of SUMO2 Modification Sites. Sci. Signal. *7*.
Toledo, L.I., Altmeyer, M., Rask, M.-B., Lukas, C., Larsen, D.H., Povlsen, L.K., Bekker-Jensen, S., Mailand, N., Bartek, J., and Lukas, J. (2013). ATR Prohibits Replication Catastrophe by Preventing Global Exhaustion of RPA. Cell *155*, 1088–1103.
Ulrich, H.D., and Walden, H. (2010). Ubiquitin signalling in DNA replication and repair. Nat. Publ. Gr. *11*.
Wu, C.-S., and Zou, L. (2016). The SUMO (Small Ubiquitin-like Modifier) Ligase PIAS3 Primes ATR for Checkpoint Activation. J. Biol. Chem. *291*, 279–290.
Wu, C.-S., Ouyang, J., Mori, E., Nguyen, H.D., Maréchal, A., Hallet, A., Chen, D.J., and Zou, L. (2014). SUMOylation of ATRIP potentiates DNA damage signaling by boosting multiple protein interactions in the ATR pathway. Genes Dev. *28*, 1472–1484.
Xiao, Z., Chang, J.-G., Hendriks, I.A., Sigurðsson, J.O., Olsen, J. V, and Vertegaal, A.C.O. (2015). System-wide Analysis of SUMOylation Dynamics in Response to Replication Stress Reveals Novel Small Ubiquitin-like Modified Target Proteins and Acceptor Lysines Relevant for Genome Stability. Mol. Cell. Proteomics *14*, 1419–1434.

Figure S1

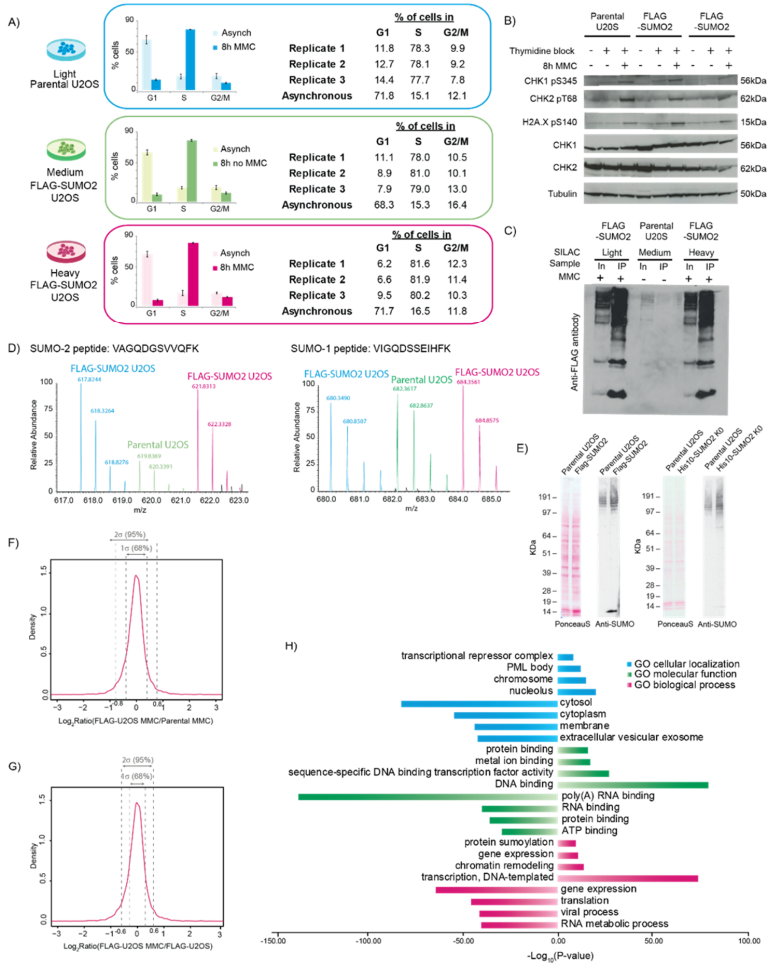

Figure S1 SUMOylation changes upon MMC treatment. Related to Figure 1. A) Flow cytometry-based cell cycle profile of SILAC labeled cells after synchronization for 24 hours with thymidine, and then released with and without 1μM MMC for 8 hours. B) Western blot of DNA damage and replication stress markers from parental and FLAG-SUMO2 U-2-OS cells after synchronization and treatment as in (A). C) Enrichment of SUMO from U-2-OS cells stably transfected with FLAG-SUMO2 and parental cells, from label swap SILAC experiment. All SILAC conditions were synchronized as in (A) and MMC treatment was performed as in (A). In: input; IP: immunoprecipitation. D) Full scan MS mass spectra of SUMO2 and SUMO1 derived SILAC peptide triplet MS intensities (relative abundance) from proteome measurements. All cells were synchronized for 24 hours with thymidine, and medium and heavy conditions were released into MMC for 8 hours while light cells were untreated. E) SUMO expression levels in untreated FLAG-SUMO2 U-2-OS (left) and His10-SUMO-2-K0-Q87R cells by western blot analysis of whole cell extracts. F) Distribution of Log_2 ratios of MMC treated FLAG-SUMO2 U-2-OS compared to MMC treated parental U-2-OS, from the unmodified peptides identified in the SUMO-enrichment MS analysis. One and two standard deviations (1σ and 2σ) from the mean are indicated with dashed lines, and used to set cutoffs for determining SUMOylated

peptides (ratio above or below 2σ). G) Distribution of Log_2 transformed ratios of MMC treated compared to untreated FLAG-SUMO2 U-2-OS of all the unmodified peptides identified in the SUMO-enrichment MS analysis. One and two standard deviations (1σ and 2σ) from the mean are indicated with dashed lines, and used to set cutoffs for determining MMC regulated and non-regulated SUMOylated peptides (ratio above or below 2σ). H) GOCC (Gene Ontology Cellular Compartments), GOMF (Molecular Functions) and GOBP (Biological Processes) enrichment performed with InnateDB from all 702 proteins deemed SUMOylated from the proteomics experiment. Related to Figure 1 and Table S1.

Figure S2

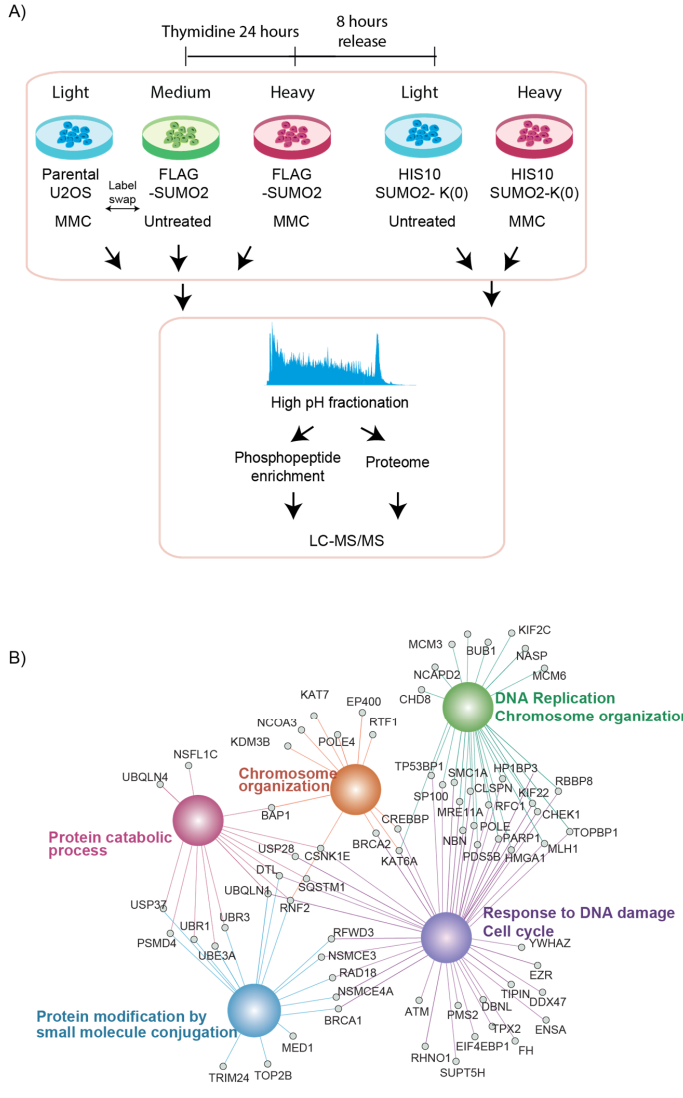

Figure S2 Phosphorylation changes in MMC treated cells. Related to Figure 2. A) Experimental design of quantitative phosphoproteomics analysis. Cells were treated equivalent to the proteomics experiments for SUMO enrichment described in Figures 1 and S1. Cells were lysed and proteins digested with trypsin prior to offline reversed-phase high-pH reversed-phase fractionation of the resulting peptides. An aliquot of each fraction was analyzed directly by LC-MS/MS for proteome measurements, whereas for phosphoproteome measurements phosphopeptides were enriched by TiO2 prior to LC-MS/MS analysis. B) Phosphoprotein network representation of enriched GOBP terms from all proteins with regulated phosphorylation sites. The colored hubs represent the enriched GOBP terms, while the small nodes indicate the proteins with these terms with significantly up-regulated phosphorylation sites upon MMC treatment. Analysis was performed with Cytoscape using the ClueGO app. Related to Figure 2 and Table S2.

Figure S3

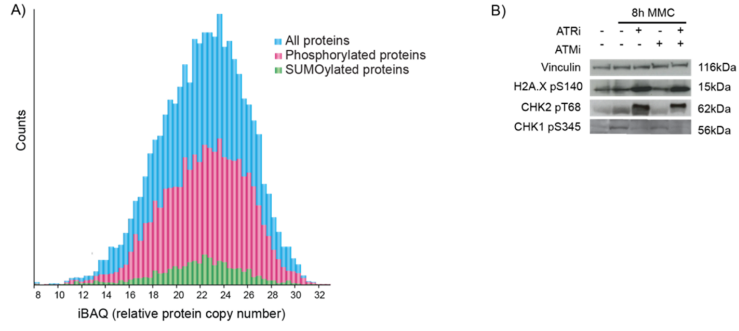

Figure S3 SUMOylation and phosphorylation data integration. Related to Figure 3. A) Distribution of the estimated relative protein copy number (iBAQ) of all proteins, phosphorylated proteins and SUMOylated proteins from datasets acquired in Figures 1 and 2. B) Western blot of markers of activity of DDR kinases ATM and ATR for cells treated with or without MMC in combinations with ATRi (ATR-45) and ATMi (KU55933). Related to Figure 3 and Table S3.

Figure S4

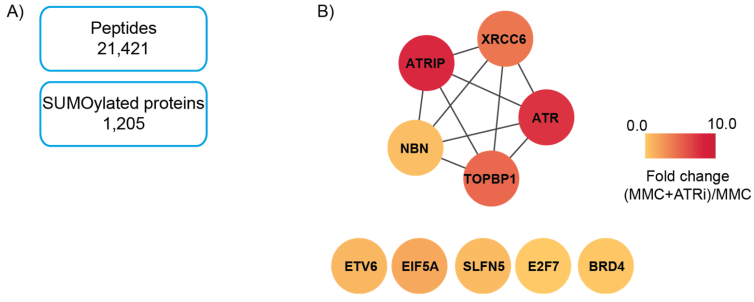

Figure S4 TOPBP1 SUMOylation regulation by ATR and ATM inhibitors. Related to Figure 4. A) Overview of the number of SUMOylated peptides and SUMO target proteins identified from the label free quantitative SUMO-2 proteomics analysis. B) Functional network analysis of proteins with significantly regulated SUMOylation after ATR inhibition. Color gradient represents the absolute fold change of the SUMO enrichment from FLAG-SUMO2 U-2-OS cells treated with MMC in combination with ATRi (ATR-45) compared to MMC only. Analysis was done with the STRING database and Cytoscape. Related to Figure 4 and Table S4.

Figure S5

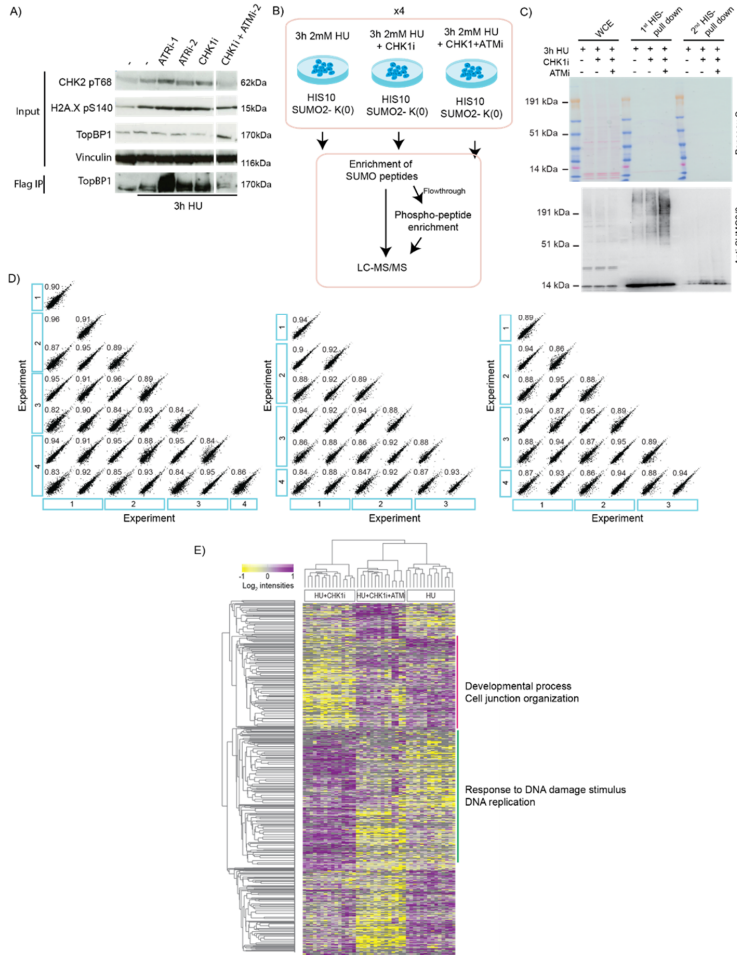

Figure S5 Integrated phosphorylation and SUMOylation analysis in RS and replication fork breakage. Related to Figure 5. A) Western blot analysis of TOPBP1 SUMOylation and markers of ATR and ATM activity upon treatment with HU with and without ATR, CHK1 and ATM inhibitors. ATRi-1: ATR-45; ATRi-2: AZ-20; CHK1i: SCH900776; ATMi-2: KU60019. B) Experimental setup for label free quantitative proteomics analysis of SUMOylation and phosphorylation substrates and sites from HIS10-SUMO2 U-2-OS cells. C) Western blot validation of SUMO enrichment from the experiments performed in (A). WCE: whole cell extract. Two sequential pulldowns were preformed, indicated as 1st and 2nd HIS-pull downs. D) Correlation of the quantification of peptides identified from the proteomics analysis, with Pearson correlation coefficients. E) Unsupervised hierarchical clustering of the 3,373 phosphorylation sites deemed to be significantly perturbed by ANOVA testing (FDR <0.05). Two clusters with enriched GOBP terms are indicated by the colored bars.

Supplemental Experimental Procedures

Cells

Human osteosarcoma U-2-OS cells (female) were kindly shared by Roeland Dirks, who acquired them from ATCC. Cell were cultured in DMEM (Gibco, Invitrogen), supplemented with 10% fetal bovine serum (FBS), 100U/mL penicillin (Invitrogen), 100µg/mL streptomycin (Invitrogen) (complete DMEM), at 37°C, in a humidified incubator with 5% CO2. For SILAC labeling (Ong, 2002), cells were cultured under the same conditions, using SILAC DMEM (Thermo Fisher Scientific) supplemented with 10% dialyzed FBS (Sigma), 100U/mL penicillin (Invitrogen), 100 µg/mL streptomycin (Invitrogen), 2 mM L-glutamine (Gibco) and one of the following three labeling combinations: 1) natural 'light' variants of the amino acids (Lys0, Arg0) (Sigma) 2) medium variants of amino acids {L-[2H4]Lys (+4) and L-[13C6]Arg (+6)} (Lys4, Arg6), and 3) heavy variants of the amino acids {L-[13C6,15N2]Lys (+8) and L-[13C6,15N4]Arg (+10)} (Lys8, Arg10). This is henceforth referred to as complete SILAC DMEM. Medium and heavy variants of amino acids were purchased from Cambridge Isotope Laboratories. We have not performed specific authentication of the cell lines used in this study.

Stable cell line generation

To generate stable cell lines for SUMO enrichment, U-2-OS cells were infected with lentivrus encoding either FLAG-tagged SUMO-2 (FLAG-SUMO2) or His10-SUMO-2-K0-Q87R (His10-SUMO2-K0), both containing a GFP sequence separated by an IRES (Schimmel et al., 2014; Xiao et al., 2015). Two weeks after infection, cells were fluorescence-sorted for a low expression level of GFP using a FACSAria II (BD Biosciences). The His10-SUMO2-K0-Q87R has the following amino acid sequence: AHHHHHHHHHHGGSMSEERPREG

VRTENDHINLRVAGQDGSVVQFRIRRHTPLSRLMRAYCERQGLSMRQIRFRFDGQPINET DTPAQLEMEDEDTIDVFRQQTGG.

Synchronization and drug treatments of cells

For thymidine blocking cells were grown to approximately 70% confluence on 15cm petri dishes (Greiner bio-one). Cells were treated with 4 mM thymidine (Sigma) in complete DMEM or complete SILAC DMEM for 24 hours and released by washing two times with PBS (Gibco, Life Technologies). For release, the media was replaced with complete DMEM or complete SILAC DMEM with or without drugs as indicated. Mitomycin C (MMC) was used at a concentration of 1 µM (Sigma) and hydroxyurea (HU) at 2 mM. Inhibitors were used at the following concentrations: ATR-45 (Ohio University) at 5 µM, AZ20 at 2µM, KU55933 (Calbiochem) at 10 µM, KU60019 (Selleckchem) at 10 µM and SCH900776 (MedKoo Biosciences) was used at 1 µM. When inhibitors were used in combination with drugs, both were added simultaneously.

Flow cytometry for cell cycle analysis

For cell cycle analysis cells were harvested with trypsin, washed two times with PBS, then fixed and permeabilized overnight at 4°C with ice cold ethanol. Cells were centrifuged at 250x*g* for 2 minutes. The pellet was resuspended in PBS complemented with 25µg/mL propidium iodide (Sigma) and 100µg/mL RNAse A (Sigma) and incubated at 37 °C for 30 minutes. FACS analysis was performed on a BD FACSCalibur (BD Biosciences), and the data was analyzed using the FlowJo software.

SUMO target protein enrichment

Cells were washed two times with PBS and lysed with lysis buffer (1% SDS, 0.5% NP-40, 50 mM sodium fluoride, 1 mM sodium orthovanadate, 5 mM β-glycerol phosphate, 0.5 mM EGTA, protease inhibitor including EDTA (Roche) and 10 mM N-ethylmaleimide (NEM)). Lysates were either used directly for further processing or snap frozen with liquid nitrogen and later thawed at 30°C. Chloroacetamide (CAA) was added to a final concentration of 55 mM. Lysates were sonicated with a microtip sonicator (Sonics Vibra Cell, VCX130) for 3 cycles of 10 seconds on and 15 seconds off at 60% amplitude. Samples were kept cool during sonication but not below 30°C to prevent SDS precipitation. Lysates were incubated for 30 minutes at room temperature then centrifuged at 13,200 rpm at 4°C for 45 minutes, and the supernatant was used for enrichment. An aliquot was kept for testing the input by western blotting. Bradford assay was used to determine protein concentration, and equal amounts of protein were used for each condition. Monoclonal Anti-FLAG M2 beads (Sigma) were washed three times with Wash buffer (50 mM Tris, 150 mM NaCl, 70 mM chloroacetamide, 0.5% NP-40, 5 mM sodium fluoride, 1 mM sodium orthovanadate, 5 mM β-glycerol phosphate, 0.5 mM EGTA, 10 mM NEM, protease inhibitor including EDTA (Roche)). An aliquot of 10 µL bead slurry was used for each milligram of protein in the sample, and samples were incubated with the beads for 90 minutes at 4ºC with rotation. Beads were collected at 500x*g* for 3 minutes, and washed five times in with Wash buffer (without CAA). FLAG-SUMO-2 conjugated proteins were eluted with tenfold bead volumes of 5% SDS in Wash buffer containing 1 mM FLAG-M2 epitope peptide (Sigma), for 10 min at room temperature with shaking. After spinning the supernatant was concentrated by transferring to an Amicon Ultra 10k NMWL spin filter (Millipore) and spinning at 7500x*g* until 50 µL remained. 10 µL NuPAGE LDS sample buffer was added, the filter was inverted, and the sample collected in a fresh tube by spinning at 2500x*g* for 2 minutes. The eluted samples were run on an SDS-Page gel for western blotting or in-gel digestion for mass spectrometry analysis.

In-gel digestion

Eluted SUMO-target enriched samples were run on a NuPage 4-12% Bis-Tris protein gel (Novex, Thermo Fisher Scientific), and stained with Colloidal Blue Staining Kit (Invitrogen). Gel pieces were excised and transferred to 1.5 ml tubes where they were destained in 50% ethanol in 25mM ammonium bicarbonate (ABC), then dehydrated in 97% ethanol with shaking. This was followed by incubation

with 10 mM DTT (in 25 mM ABC) for 30 minutes and for an additional 30 minutes with 55 mM CAA (in 25 mM ABC). Samples were washed twice with 25mM ABC with shaking for ten minutes, and again dehydrated with 96% ethanol. Trypsin (Sigma) was added (1.5 µg/mL) for one hour with subsequent addition of an equal volume and incubated overnight with shaking. Trypsin activity was quenched by acidifying the sample with trifluoroacetic acid (TFA) to a final concentration of 1%. The sample was collected, and the remaining gel was sequentially washed with Washing solution A (30% (v/v) acetonitrile (ACN), 3% (v/v) TFA in milliQ), then Washing solution B (80% (v/v) ACN, 0.5% (v/v) acetic acid in milliQ) and finally with 100% ACN. The sample was collected after incubation with each solution for 30 minutes with shaking. Samples were prepared for loading on C-18 stage-tips (Rappsilber et al., 2007) by concentrating and removing ACN with vacuum centrifugation.

SUMO-peptide enrichment

Thirty 15cm petri dishes at 80% confluence with U-2-OS cells expressing His10-SUMO-2-K0-Q87R (approximately 15 million cells per dish) were used for each condition to identify SUMO-2 sites. We employed our previously established SUMO site enrichment method (Hendriks and O Vertegaal, 2016; Hendriks et al., 2014). Cells were washed three times with ice-cold PBS on the plate. After the last wash 2mL ice-cold PBS was added to each plate, cells were scraped and collected in 15 mL tubes. Cells were spun down at 250x*g* and re-suspended in ice-cold PBS. Small aliquots of cells (~80,000 cells) were kept and lysed in lysis buffer (1% NP-40, 2% SDS, 150 mM NaCl, and 50 mM TRIS, buffered at pH 7.5) for control western blotting. All PBS was aspirated from the main batches of cells. Cell pellets were collected and subsequently lysed in 10 pellet volumes of lysis buffer (6 M guanidine-HCl, 100 mM sodium phosphate, 10 mM TRIS, buffered at pH 8.0). Lysates were sonicated using a microtip sonicator at 30 Watts for ten seconds of sonication time per 10 mL lysate. Sonication steps were repeated once and tubes were inverted to mix in between sonication steps. Protein quantities from the lysates were equalized using the bicinchoninic acid assay. Next, lysates were supplemented with imidazole and β-mercaptoethanol to a final concentration of 50 mM and 5 mM respectively. Ni-NTA agarose beads (Qiagen) at 20 µL (dry volume) per 1 mL lysate were used for SUMO purification. Following overnight incubation at 4°C, beads were centrifuged at 500x*g* for 2 minutes, and washed using at least 5 bead volumes of wash buffers 1-4 in the following order: wash buffer 1: 6 M guanidine-HCl, 10 mM TRIS, buffered at pH 8.0, 100 mM sodium phosphate, 0.1% Triton X-100, 10 mM imidazole, 5 mM β-mercaptoethanol; wash buffer 2: 8 M urea, 10 mM TRIS, buffered at pH 8.0, 100 mM sodium phosphate, 0.1% Triton X-100, 10 mM imidazole, 5 mM β-mercaptoethanol; wash buffer 3: 8 M urea, 10 mM TRIS, buffered at pH 6.3, 100 mM sodium phosphate, 10 mM imidazole, 5 mM β-mercaptoethanol; wash buffer 4: 8 M urea, 10 mM TRIS, buffered at pH 6.3, 100 mM sodium phosphate, 5 mM β-mercaptoethanol. Subsequently, all wash buffer was aspirated entirely, and proteins were eluted using one bead volume of elution buffer (7 M urea, 10 mM TRIS, buffered at pH 7.0, 100 mM sodium phosphate, 500 mM imidazole) for at least 30 minutes. Elution steps were repeated twice. All

eluted fractions were pooled and filtered using 0.45 micron filters (twice pre-washed with Elution Buffer) to clear any remaining beads from the samples. The flow through from this pull down can be used for enrichment of phosphorylated peptides after trypsin digestion. For mass spectrometric analysis of SUMOylated peptides, samples were concentrated using 100 kDa cut-off spin filters (pre-washed with elution buffer), using a temperature-controlled centrifuge set to 20°C and centrifuging at 8,000x*g*. After concentration, filters were washed again using 250 µL of elution buffer without imidazole. Concentrated SUMOylated proteins were removed from the filters by centrifuging the filters while placed upside down into an open 1.5 mL LoBind tube. The concentration of purified SUMOylated proteins was determined using the Bradford assay (BioRad). SUMOylated proteins were digested using sequencing grade endoproteinase Lys-C in a 1:25 (w/w) enzyme-to-protein ratio for 4 hours. Subsequently, 10 mM β-mercaptoethanol was freshly added and the samples were further digested overnight by an additional amount of Lys-C equal to the first amount. All digestion steps were performed in the dark at room temperature. Protein samples were subsequently transferred to 15 mL tubes and diluted with half the amounts of guanidine lysis buffer used to lyse the initial cell pellets and were supplemented by adding imidazole to a final concentration of 50 mM and β-mercaptoethanol to a final concentration of 5 mM. Ni-NTA agarose beads at 40 µL (dry volume) per 1 mL sample were used for SUMO enrichment. Following incubation at 4°C for 5 hours, beads were centrifuged at 500x*g* for 2 minutes and washed again with wash buffer 1- 4 as described before. Proteins were eluted using one bead volume of elution buffer (7 M urea, 100 mM sodium phosphate, 10 mM TRIS, buffered at pH 7.0, 500 mM imidazole). All eluted samples were passed through 0.45 µM filters (twice pre-washed with elution buffer) to remove the remaining beads from the samples. Next, samples were concentrated by passing them through 10 kDa cut-off spin filters (pre-washed with elution buffer) at 14,00x*g* at 20°C. After concentration, the peptides remaining on the filters were washed twice with 250 µL of elution buffer without imidazole, and re-concentrated. Final concentrated SUMOylated peptides were removed from the filters by centrifuging the filters while placed upside down into a 1.5 mL LoBind tube. The double-purified SUMOylated peptides were trypsin digested, purified on stage-tips and analyzed by mass spectrometry to map specific sites of protein SUMOylation.

Sample preparation for phospho-peptide enrichment

Samples for phospho-peptide enrichment were either prepared freshly as described here or taken from the flow-through after the first HIS-based enrichment in the SUMO-peptide enrichment procedure (and directly trypsin digested as described below). For lysate preparation, cells were washed twice with PBS and subsequently lysed on the plate with boiling (99°C) lysis buffer (6 M guanidinium hydrochloride (GndCl), containing 5 mM tris(2carboxyethyl)phosphine (TCEP) and 10 mM CAA in 100 mM Tris, pH 8.5). The lysate was collected by scraping and subsequently further boiled for 10 minutes at 99°C prior to microtip sonication on a Sonics Vibra Cell (VCX130) at amplitude 50%, for two minutes with 1 second on and 1 second off pulses. Protein concentrations were estimated using Bradford assay (Bio-

Rad). For SILAC samples equal amounts of protein were mixed at this point, and for label free equal amounts of protein were used separately for further processing. Samples were digested with Lys-C in an enzyme:protein ratio of 1:100 (w/w) for 4 hours at 25 °C. GndCl was diluted to 2 M using 25 mM Tris pH 8.5, and the samples were further digested with trypsin (Sigma Aldrich) at 1:100 (w/w) overnight at 37 °C with slow shaking. Trypsin activity was quenched by acidifying the sample with TFA to a final concentration of 1%. The peptide mixtures were desalted and concentrated on a C18-SepPak cartridge (Waters). Sep-Pak columns were washed with 100% ACN and 0.1% TFA buffer before loading the sample, and the column were then washed with 0.1%TFA and stored at 4°C. Peptides were eluted from with 2 mL 40% ACN in 0.1% TFA, and then with 2 mL 60% CAN in 0.1% TFA followed by concentration and removal of ACN by vacuum centrifugation for 40 minutes at 45°C. Peptide concentration in the resulting sample as measured at 280 nM absorbance on a Nanodrop (Thermo Fisher Scientific). The eluted samples were either used directly for phospho-peptide enrichment fractionated as described below prior to further processing.

Offline High pH Reversed-Phase HPLC Fractionation

The eluted and concentrated peptide samples were separated using an Ultimate 3000 high-pressure liquid chromatography (HPLC) system (Dionex) on a C_{18} Waters Xbridge BEH130 column (3.5 µm 4.6 × 250 mm). Peptides were separated and collected as described previously (Batth et al., 2014). Buffer A (milli-Q water), buffer B (100% ACN), and buffer C (50 mM ammonium hydroxide) were operated simultaneously at a final flow rate of 1 ml/min. Buffer C was operated throughout the separation gradient at 0.1 ml/min. The separation gradient consisted of increasing B from 5% to 25% in 65 minutes. Buffer B was increased to 35% in 10 minutes and 60% in 5 minutes followed by a sharp increase to 90% B in 2 minutes where it was held for additionally 5 minutes. The column was re-equilibrated to starting conditions with a 2 minute ramp down to 5 % buffer B where it was held 6 minutes prior to injection of the next sample. Fractions were collected at 1 minute intervals in a 96 deep well plate using automated fraction collector-3000 coupled to the HPLC system. Fractions were collected until the 80 minute mark in the gradient and manually concatenated to 14 fractions.

Phospho-peptide enrichment

Following fractionation, phospho-peptides were enriched from each fraction, or for enrichment after SUMO-peptide enrichment, samples were directly after Sep-Pak elution as described above.

Titanium dioxide (TiO_2) beads (5 µm Titansphere, GL Sciences) (Larsen, 2005; Olsen et al., 2006) were incubated in 20 mg/ml of 2, 5-dihydroxybenzoic(DHB) acid in 80% ACN and 6% TFA before use. TiO_2 bead slurry was prepared at 20 mg beads per ml DHB solution. Prior to adding the TiO_2 beads, each of the 14 fractions was diluted two-fold with 100% ACN in 12% TFA. 20 µL of TiO_2 beads slurry was added to each of the 14 fractions followed by 15 minutes incubation at room temperature with rotation. A second incubation was done by pooling fractions 1 to 5, 6 to 9 and 10 to 14. These were

incubated with 40 µl of the TiO_2 DBH slurry for another 15 min with rotation. Samples were centrifuged at 4000x*g* for 5 minutes and supernatant was removed. The beads were loaded on C8 tips (Empore) and washed on-tip with 10% ACN in 6% TFA, followed by 40% ACN in 6% TFA and finally 80% ACN in 6% TFA (Jersie-Christensen et al., 2016). Phospho-peptides were eluted first with 20 µL of 5% NH_4OH followed by 20 µL of 10% NH_4OH with 25% ACN. Eluted peptides were concentrated by vacuum centrifugation and loaded onto C-18 stage-tips.

Electrophoresis and immunoblotting

For Western Blot analysis of SUMOylated proteins enriched from His10-S2-K0 expressing U-2-OS cells, whole cell extracts or purified protein samples (procedures described above) were separated on Novex Bolt 4-12% Bis-Tris Plus gradient gels using MOPS buffer and transferred onto Hybond-C nitrocellulose membranes (GE Healthcare Life Sciences) using a submarine system (Life Technologies). Membranes were stained with Ponceau S (Sigma) to stain total protein and blocked with PBS containing 8% milk powder (w:v) and 0.05% Tween-20 (v:v) before incubating with the primary antibodies.

For analysis of total protein expression, phosphorylated proteins lysates were prepared as described below and SUMO enrichment from FLAG-SUMO2 expressing cells lysates from procedures described above were used. Cells were washed twice in ice-cold PBS, and lysed in complete modified RIPA buffer (50mM Tris, pH 7.5, 150mM NaCl, 1% NP-40, 0.1% sodium deoxycholate, 1 mM EDTA, 5 mM β-glycerolphosphate, 5 mM NaF, 1 mM sodium orthovanadate, complete inhibitor cocktail tablet (Roche)). Lysates were cleared by centrifugation at 13,000x*g* for 15 minutes. Protein concentration was measured using Bradford assay and lysates were boiled in NuPAGE LDS sample (Invitrogen) buffer with DTT for 15 minutes. Proteins were resolved on NuPAGE Novex 4-12% gradient Bis-Tris gels (Invitrogen) and transferred onto nitrocellulose membranes. After blocking for 1 hour in 5% skimmed milk (w:v) or 5% BSA (w:v) in PBS supplemented with 0.1% Tween-20 (PBST) (v:v), the membranes were incubated with primary antibodies in blocking solution overnight at 4°C. Blots were incubated with horse radish peroxidase coupled secondary antibody (Jackson Immunoresearch) in 5% skimmed milk in PBST. Detection was performed with Novex ECL chemiluminescent Substrate Reagent Kit (Invitrogen).

Nanoflow LC–MS/MS

For LC-MS/MS analysis, STAGE-tips were eluted twice with 10 µl 40% ACN in 0.5% formic acid. All samples were analyzed on an Easy-nLC 1000 system coupled to the Q Exactive HF instrument (Thermo Fisher Scientific) through a nanoelectrospray ion source. Peptides were separated on an analytical column (inner diameter 75 µm), with 1.9 µm C_{18} beads (Dr. Maisch, packed in-house) with a flow rate of 250nL/min at 40°C using an integrated column oven (PRSO-V1, Sonation GmbH). The spray voltage was set to 2kV, s-lens RF level to 50 and the heated capillary to 275°C. The mass spectrometer was operated in data-dependent acquisition (DDA) mode, in positive polarity mode with 30 seconds

dynamic exclusion window. Full scan resolution was set to 60,000, scan range to m/z 200-2000 and full-MS ion target value was 3e6. All fragmentation was performed by higher-energy collisional dissociation (HCD) with parallel acquisition. For enriched SUMO-peptides and SUMO-targets, as well as phospho-peptide enriched samples from Figure 1, the peptides were separated on a 15 cm analytical column with a 95 minute gradient from 8% to 75% CAN in 0.1% formic acid. For SUMO-target enriched samples from Figure 4, the gradient was run over 59 minutes. All samples were run with a top 7 method. For enriched SUMO- and phospho-peptides in Figure 5, the samples were run on a 50cm column with a 264 minute gradient from 8% to 75% ACN in 0.1% formic acid. A top 10 MS/MS method was utilized for analysis of these samples.

Quantification and statistical analysis

Raw Data Processing and Analysis

All raw LC–MS/MS data was analyzed by MaxQuant software suite v1.4.1. or v1.5.11. using the Andromeda Search engine. The searches were performed against the complete human UniProt database. The default contaminant protein database was included and identifications from this source were excluded during analysis of the data. We used the "match between runs" option. Cystein carbamidomethylation was set as a fixed modification while methionine oxidation, protein N-terminal acetylation, and pyro-glutamate formation from glutamine were set as variable modifications. For identification of SUMOylated peptides SUMOylation remnant (QQTGG) with monoisotopic mass of 471.20776 Da and pyroSUMOylation (pyroQQTGG) remnant with monoisotopic mass of 454.18121 Da modification on lysine residues was set as a variable modification. Similarly, phosphorylation of serine, threonine, and tyrosine residues were set as variable modifications for identification of phosphorylation sites. Using the target-decoy strategy the false discovery rate (FDR) was set to 1% for peptide spectral matches (PSM) and protein identification. For each experimental setup the raw MS data was analyzed in a separate MaxQuant analysis. When analyzed together each experiment was processed in separate parameter groups. Mapping of proteins with modifications sites is based on the identified sequence, and protein inference is performed on the global level applying information form peptides identified from all raw MS data. This latter approach was applied for MMC treated FLAG-SUMO2 IPs, HIS10 SUMO2-K(0) IPs, phosphoproteome and proteomes from Figures 1, S2, 2 and S2.

Bioinformatics analysis

Functional protein interaction networks were mapped using the STRING database (Szklarczyk et al., 2015) and further processed with Cytoscape (www.cytoscape.org). For network mapping a minimum confidence score of 0.4 was required. Clusters of highly interconnected nodes within the networks were extracted using the MCODE Cytoscape app. Analysis to identify enrichment of Gene Ontologies (GO) were done using InnateDB (Lynn et al., 2008) and P-values were corrected for multiple testing with by Benjamini Hochberg FDR. Hierarchical clustering, as well as ontology enrichment of clusters, was done

using Perseus (Tyanova et al., 2016). For the clustering illustrated in Figures 5 and S5, at least three quantifications were required in at least one condition. From these we performed a multiple sample t-test using ANOVA with an FDR threshold of 0.05. Normalization was performed by subtracting the median intensity for each condition. Unsupervised hierarchical clustering was performed on the targets that were found significant. Rows were clustered using the Canberra approach and columns by Pearson correlation.

Analysis for enriched sequence motifs for the PTM enriched data was performed using IceLogo (Colaert et al., 2009), and overrepresentation was scored with fold-change with a p-value cutoff of 0.01 or 0.05, using the complete acquired dataset (non-regulated or non-modified) as the reference.

Resource Table

REAGENT or RESOURCE	SOURCE	IDENTIFIER
Chemicals, Peptides, and Recombinant Proteins		
DMEM	Gibco	31966-047
SILAC DMEM	Thermo Fisher Scientific, PAA	PAA-EL15-086
FBS (heat-inactivated)	Gibco	10270-106
Dialyzed FBS	Sigma Aldrich	F0392-500ML
Pen/strep	Gibco	15140-122
Trypsin-EDTA (0.05%)	Gibco	25300-054
L-Glutamine	Gibco	25030-024
L-Arginine monohydrochloride	Sigma Aldrich	A6969
Poly-D-lysine hydrobromide	Sigma Aldrich	P7280
L-Lysine:2HCL (13C, 99%; 15N2, 99%)	Cambridge Isotope Labs	CNLM-290-H
L-Lysine:2HCL (4,4,5,5-D5, 96-98%)	Cambridge Isotope Labs	DLM-2640-0
L-Arginine:HCL (13C6, 99%; 15N4, 99%)	Cambridge Isotope Labs	CNLM-539-H
L-Arginine:HCL (13C6, 99%)	Cambridge Isotope Labs	CNLM-2265-H
PBS	Gibco	20012-068
Thymidine	Sigma Aldrich	T9250
Mitomycin C	Sigma Aldrich	M4287
Hydroxyurea	Sigma Aldrich	H8627
Guanidine hydrochloride	Sigma Aldrich	G3272
ATR-45	Ohio State University	N/A
AZ20	Selleckchem	S7050
KU55933	Calbiochem	118500
KU60019	Selleckchem	S1570
SCH900776	MedKoo Biosciences	118500
Propidium iodide	Sigma Aldrich	P4170
TCEP	Sigma Aldrich	C4706
CAA	Sigma Aldrich	22790
Quick Start Bradford 1X Dye Reagent	BioRad	500-0205
REAGENT or RESOURCE	**SOURCE**	**IDENTIFIER**
ANTI-FLAG® M2 Affinity Gel	Sigma Aldrich	A2220
FLAG peptide	Sigma Aldrich	F3290
Trizma base	Sigma Aldrich	T1503
Complete mini EDTA-free protease inhibitor cocktail	Roche	04693124001
Trypsin	Sigma Aldrich	T6567
Lys-C	Wako Chemicals	129-02541

Endoproteinase Lys-C, Sequencing Grade	Promega	V1071
TFA	Sigma Aldrich	T6508
Acetonitrile	Merck	1.00030.2500
Ammonium bicarbonate	Sigma Aldrich	09830
5µM Titansphere	GL Sciences	GS 502075000
2,5-dihydroxybenzoic acid	Sigma Aldrich	85707
Ammonia solution 25%	Merck	1054321011
Amicon Ultra Centrifugal Filter Unit	Millipore	UFC900396
NuPAGE LDS sample buffer 4x	Novex	NP0007
1.0mm x 10 well NuPAGE 4-12% Bis-Tris Gel	Novex	NP032BOX
Amersham Hybond ECL nitrocellulose membrane	GE Healthcare	RPN303D
Novex Bolt 4-12% Bis-Tris Plus gel	Life Teachnologies	BG04125BOX
Colloidal Blue staining kit	Invitrogen	LC-6025
SepPak Classic C18 cartridges	Waters	WAT051910
C18 Column, 130Å, 3.5 µm, 4.6 mm X 250 mm	XBridge PST	186003570
2, 5 Dihydroxybenzoic acid	Sigma Aldrich	85707-1G-F
C18 (Octadecyl) 47mm	Empore	2215
C8 47 mm Extraction Disk	Empore	2214
Monoclonal ANTI-FLAG® M2 antibody	Sigma Aldrich	F1804
ReproSil-Pur 120 C18-AQ, 1.9 µm	Dr. Maisch	r119.aq
Ni-NTA beads	Qiagen	30210
Pierce BCA protein Assay Kit	Thermo Scientific	23227
Vivacon 500 Filter - 100,000MWCO	VN01H41	SartoriusStedim
VIVACON500 Filter - 10,000MWCO	VN01H01	SartoriusStedim
REAGENT or RESOURCE	**SOURCE**	**IDENTIFIER**
TopBP1 antibody	Bethyl Laboratories	A300-111A
Anti-Chk1 (phospho S345) antibody	Abcam	ab47318
Chk1 (2G1D5) Mouse mAb	Cell Signaling Technology	2360
Phospho-Chk2 (Thr68) Antibody	Cell Signaling Technology	2661
Chk2 (1C12) Mouse mAb	Cell Signaling Technology	3440
Phospho-Histone H2A.X (Ser139) Antibody	Cell Signaling Technology	2577
Histone H2A.X Antibody	Cell Signaling Technology	2595
BRCA1 Antibody	Cell Signaling Technology	9010
Anti-Vinculin antibody, Mouse monoclonal	Sigma Aldrich	V9264
Anti-RPA32/RPA2 antibody [9A1]	Abcam	ab125681

mouse monoclonal anti-SUMO-2/3	Abcam	Ab81371
Deposited Data		
Raw and analyzed data		PXD006361
Experimental Models: Cell Lines		
U-2-OS	Roeland Dirks (Leiden)	
Software and Algorithms		
MaxQuant 1.5.3.6		http://www.coxdocs.org/doku.php?id=maxquant:start
R software		https://www.r-project.org/
String v10		http://string-db.org/
Cytoscape		www.cytoscape.org
IceLogo		http://iomics.ugent.be/icelogoserver/index.html
Perseus		http://www.perseus-framework.org

Supplemental References

Batth, T.S., Francavilla, C., and Olsen, J. V. (2014). Off-line high-pH reversed-phase fractionation for in-depth phosphoproteomics. J. Proteome Res.

Colaert, N., Helsens, K., Martens, L., Vandekerckhove, J., and Gevaert, K. (2009). Improved visualization of protein consensus sequences by iceLogo. Nat. Methods *6*, 786–787.

Hendriks, I.A., and O Vertegaal, A.C. (2016). A high-yield double-purification proteomics strategy for the identification of SUMO sites. Nat. Publ. Gr. *11*.

Hendriks, I.A., D'Souza, R.C., Yang, B., Verlaan-de Vries, M., Mann, M., and Vertegaal, A.C. (2014). Uncovering global SUMOylation signaling networks in a site-specific manner. Nat Struct Mol Biol *21*, 927–936.

Jersie-Christensen, R.R., Sultan, A., and Olsen, J. V. (2016). Simple and Reproducible Sample Preparation for Single-Shot Phosphoproteomics with High Sensitivity. (Springer, New York, NY), pp. 251–260.

Larsen, M.R. (2005). Highly Selective Enrichment of Phosphorylated Peptides from Peptide Mixtures Using Titanium Dioxide Microcolumns. Mol. Cell. Proteomics *4*, 873–886.

Lynn, D.J., Winsor, G.L., Chan, C., Richard, N., Laird, M.R., Barsky, A., Gardy, J.L., Roche, F.M., Chan, T.H., Shah, N., et al. (2008). InnateDB: facilitating systems-level analyses of the mammalian innate immune response. Mol. Syst. Biol. *2*.

Olsen, J. V, Blagoev, B., Gnad, F., Macek, B., Kumar, C., Mortensen, P., and Mann, M. (2006). Global, In Vivo, and Site-Specific Phosphorylation Dynamics in Signaling Networks. Cell *127*, 635–648.

Ong, S.-E. (2002). Stable Isotope Labeling by Amino Acids in Cell Culture, SILAC, as a Simple and Accurate Approach to Expression Proteomics. Mol. Cell. Proteomics *1*, 376–386.

Rappsilber, J., Mann, M., and Ishihama, Y. (2007). Protocol for micro-purification, enrichment, pre-fractionation and storage of peptides for proteomics using StageTips.

Schimmel, J., Eifler, K., Otti Sigurðsson, J., Cuijpers, S.A., Hendriks, I.A., Verlaan-de Vries, M., Kelstrup, C.D., Francavilla, C., Medema, R.H., Olsen, J. V, et al. (2014). Molecular Cell Resource Uncovering SUMOylation Dynamics during Cell-Cycle Progression Reveals FoxM1 as a Key Mitotic SUMO Target Protein. Mol. Cell *53*, 1053–1066.

Szklarczyk, D., Franceschini, A., Wyder, S., Forslund, K., Heller, D., Huerta-Cepas, J., Simonovic, M., Roth, A., Santos, A., Tsafou, K.P., et al. (2015). STRING v10: protein-protein interaction networks, integrated over the tree of life. Nucleic Acids Res. *43*, D447-52.

Tyanova, S., Temu, T., Sinitcyn, P., Carlson, A., Hein, M.Y., Geiger, T., Mann, M., and Cox, J. (2016). The Perseus computational platform for comprehensive analysis of (prote)omics data. Nat. Methods.

Xiao, Z., Chang, J.-G., Hendriks, I.A., Sigurðsson, J.O., Olsen, J. V, and Vertegaal, A.C.O. (2015). System-wide Analysis of SUMOylation Dynamics in Response to Replication Stress Reveals

Novel Small Ubiquitin-like Modified Target Proteins and Acceptor Lysines Relevant for Genome Stability. Mol. Cell. Proteomics *14*, 1419–1434